PETROGENETIC DESCRIPTION AND 3D-MODELLING OF BRUCITE MINERALIZATION IN THE GÅSGRUVAN MARBLE QUARRY, WESTERN BERGSLAGEN

Master`s thesis in Geology and Mineralogy
Faculty of Science and Engineering
Åbo Akademi University
Cassandra af Hällström, 38086
Supervisors: Kaisa Nikkilä (ÅAU) and
Magnus Johansson (SMA Mineral AB)

TURKU 2018

af Hällström, Cassandra, 2018. *Petrogenetic description and 3D-modelling of brucite mineralization in the Gåsgruvan marble quarry, Western Bergslagen.* Master's thesis in Geology and Mineralogy for Master of Science degree. **73 pages, 39 figures, 4 tables and 5 appendices.**

This thesis is conducted in cooperation with Gåsgruvan Kalcit AB, SMA Mineral AB and Åbo Akademi University.

ABSTRACT

The Gåsgruvan quarry is located as a marble lens in the magmatic Bergslagen region in central Sweden. The deposit is hosted by 1.9-1.88 Ga Svecokarelian felsic metavolcanics and is exposed to igneous intrusions of different generations. SMA Mineral AB is currently mining coarse-grained calcite marble in Gåsgruvan for industrial use. Gåsgruvan has been subjected to mineralization of the hydroxide mineral brucite, which interferes with the floatation liquids during marble refining. Isochemical contact metamorphism between dolomitic marble and igneous intrusions, and retrograde serpentinization of Mg-rich forsterite have formed brucite.

All accessible drill cores have been relogged with the aim to determine and correlate brucite-rich zones within the Gåsgruvan deposit and to interpret the local petrogenetic origin. A 3D-model has been composed in order to demonstrate the general distribution of brucite. Complementary field mapping has been carried out within the quarry and its surroundings. Cross section profiles provided by SMA Mineral AB are utilized to study the relation between brucite and associated mineralizations. Petrographic and SEM-EDS analysis have been conducted with the aim to identify mineral assemblages and to study micro-scale relations.

Results show that brucite is concentrated in a crescent structure in the southern and southeastern deposit. Here brucite is formed by hydration of complex igneous and skarn intercalations. Brucite follows a curving pattern from southeast towards northwest and occurs in the contact of large, pre-peak metamorphic amphibolite at the western and southeastern margin. Smaller zones of brucite appear very scattered throughout the deposit, especially in the northern and central parts, where dolomite has assumedly been more abundant. In addition, some north-south striking shear zones have carried external fluids into the system and hydrated the deposit. The thesis is written in cooperation with SMA Mineral AB and Gåsgruvan Kalcit AB.

Relevant search words: *Gåsgruvan, brucite, serpentinization, dedolomitization, skarn, micro-scale analysis, 3D-model*

TABLE OF CONTENTS

ACKNOWLEDGEMENTS

First and furthermost I want to thank my supervisor Magnus Johansson for providing me with this interesting and worthwhile topic. I express gratitude to my supervisor Kaisa Nikkilä at Åbo Akademi University and to Karin Högdahl at Uppsala University and Rikke Vestergaard at Aarhus University for insightful and constructive ideas for my thesis. SMA Mineral AB and Åbo Akademi University receive my warm gratitude for aiding me with field work material and additional support. I also want to thank all friends and family who thought of me and encouraged me during this writing process.

Matias, I am eternally indebted to you for your unconditional support, encouragement and belief in me.

SVENSK SAMMANFATTNING

Gåsgruvan är belägen i västra Bergslagen i centrala Sverige. SMA Mineral AB bryter kalcitrik och grovkornig marmor i Gåsgruvans dagbrott för industriellt bruk. Marmoravlagringen är ca 1400 meter lång, 50–250 meter bred och har påvisats sträcka sig till ett djup på åtminstone 270 meter. Marmorlinsens strykning är nordvästlig och stupningen är nästintill vertikal. Två skjuvzoner skär Gåsgruvan i nord-sydlig riktning och består främst av talk-kloritskiffer. Gåsgruvan är utsatt för mineralisering av hydroxidmineralet brucit. Bruciten har påvisats vara ett problem eftersom mineralets hydroxidgrupp höjer flotationsvätskornas pH-värde, vilket resulterar i en sämre anrikningsprodukt. Geokemisk analys visar att brucitrik marmor består av ca 20 % MgO.

Bergslagen är en magmatisk provins som formats på kontinentalskorpa i en extensionspräglad omgivning, troligen i en back-arc bassäng. Bergslagen är belägen i den Svekokarelska orogenin som tillhör den Fennoskandiska skölden. Gåsgruvans marmorlins ligger i en ca 1,9–1,88 Ga felsisk, metavulkanisk succession med ryolitisk och/eller dacitisk sammansättning. Metavulkaniten är över- och underlagrad av metasedimentära bergarter, och en del metavulkaniska bergarter är även inlagrade i metasedimenten. Metavulkaniten har omvandlats i samband med magnesiumalterering innan regionalmetamorfos. Dolomit- och kalcitrika marmoravlagringar förekommer sporadiskt i Bergslagen. En del av marmorn har definierats som kemiskt sedimentära bergarter och en del härstammar från stromatoliter där ursprungsformen delvis bevarats. Den övre vulkaniska successionen karakteriseras av regionalsättning samt avlagring av vulkaniska och karbonatrika bergarter, där även metalliska mineralavlagringar förekommer.

Den Svekokarelska orogenin påverkades av regional- och kontaktmetamorfos vid 1,85–1,8 Ga. Bergarterna deformerades plastiskt under två metamorfosskeden i grönskiffer- och amfibolitfacies. De södra delarna av Bergslagen präglades även lokalt av granulitfacies. De orogena bergarterna genomslogs senare av mafiska och felsiska gångbergarter. Tre omvandlade amfibolitgångar med en nordvästlig strykning intruderar Gåsgruvan och har associerats med de felsiska metavulkaniterna. I nordost

bemöts Gåsgruvan av synvulkanisk Horrsjö-granit. Marmorn och de metalliska mineralavlagringarna är associerade med skarn. Skarn har formats då kalkrika och suprakrustala successioner påverkats av regionalmetamorfos. Skarn har även bildats i samband med fluidalterering från intrusiva bergarter. Skarn i Gåsgruvan är pyroxen- och granatrikt, samt delvis magnesiumaltererat. Yngre plutoniska bergarter förekommer i Gåsgruvans närregion, och är anslutna till det 1,85–1,67 Ga Transskandinaviska magmatiska bältet (TIB). TIB-relaterad, porfyrisk Filipstads granit infinner sig söder om Gåsgruvan. De yngsta TIB-intrusionerna representeras av diabasgångar från två generationer. Norr om Gåsgruvan förekommer en diabasgång vars ålder sammanfaller med den Svekonorvegiska orogenin.

Brucit är ett hydroxidmineral med den kemiska formeln [$Mg(OH)_2$]. Mineralet uppträder i flera färger men rödbruna varianter tyder på hög manganhalt. Brucit i Bergslagen har sammanträffats främst i Värmland och i stora sulfidavlagringar i öst. Mineralet formas i karbonatstenar i låga temperaturer då hydrotermala fluider tränger sig in i karbonaten. Brucit förekommer även i klorit- och talkskiffer och i serpentiniserade bergarter. Mineralet förekommer sällan i silikatrika omständigheter. Gåsgruvans brucit har huvudsakligen formats under kontaktmetamorfos mellan dolomitrik marmor och intrusiva bergarter som frigett värme. Under denna dedolomitisering har dolomiten omvandlats till mineralet periklas. Periklasen har senare hydrerats till brucit under det sista metamorfosskedet vid T=≤600°C. En del periklaskärnor har bevarats i brucitkornen eftersom reaktionen inte fullbordats. Brucit har även formats som en reaktionsprodukt vid serpentinisering. Under serpentinisering hydreras den magnesiumrika olivinkomponenten forsterit. I gengäld bildar den järnrika komponenten mineralet magnetit som ofta förekommer som en kärna i brucit. Förekomsten av mineralen forsterit, spinell och diopsid indikerar att gruvan varit utsatt för temperaturer över 600°C.

Avhandlingens syfte var att undersöka distributionen av brucit inom hela gruvfältet, samt att förstå de lokala mineraliseringar och hydrotermala omvandlingar som gett upphov till brucitförekomsten. Kartering utfördes på alla tillgängliga borrkärnor och arbetet kompletterades med fältkartering. Gåsgruvan delades in i nio petrologiskt varierande zoner. Alla karterade brucitstråk korrelerades samman och den tolkade brucitfördelningen demonstrerades vidare med en generaliserad 3D-modell.

3D-modellen konstruerades med karteringsdata och med kärnintervall där MgO/SiO_2-förhållandet överskred ett. Det här förhållandet framhävde magnesiumrika och silikatfattiga mineral såsom brucit.

Femton tunnslip preparerades från brucitrika samplar som valdes från borrkärnor och fältområden. Tunnslipen undersöktes med petrografiskt mikroskop och svepelektronmikroskop för att identifiera mineral och texturer. Analys med svepelektronmikroskop gav endast semikvantitativa resultat och jämfördes följaktligen med referensdata. Litologiska profiler konstruerades för att undersöka relationen mellan brucit och associerade mineraliseringar. Resultaten tillämpades för tolkning av brucitens distribution i gruvan och för att definiera brucitens lokala, petrogenetiska ursprung.

Resultaten visar att bruciten är främst koncentrerad i gruvans södra och sydöstra delar i en halvcirkelformad struktur. Denna struktur sträcker sig långt in i berggrunden och fortsätter troligtvis mot söder. Bruciten sträcker sig vidare från sydost till nordväst i en slingrande struktur. I de södra delarna är bruciten associerad med både serpentinisering och dedolomitisering, och en del inlagrad metavulkanit förekommer här. I sydöstra gruvan är bruciten sammankopplad med amfibolit, medan den yngre diabasgången i öst troligtvis inte är associerad med brucitförekomsten. I öst förekommer bruciten främst som ljusa, rundade pseudomorfa korn. Den pseudomorfa texturen indikerar att bruciten härstammat från periklas. Vid de övre delarna präglas marmorn av kloritisering vilket tyder på retrograd skarnalterering. Bruciten befinner sig även i nära kontakt med skjuvzoner som troligen infört vattenrika fluider till avlagringen. I västra delen är bruciten associerad med skarn och järnoxider. I nordvästra gruvan är bruciten däremot väldigt järnrik och brun, och förekommer främst intill en amfibolitkontakt tillsammans med spinell. I de norra och centrala delarna är bruciten distribuerad i ett sporadiskt nätverk som inte följer ett förutsägbart mönster. Detta kan bero på att dolomithalten varierat i avlagringen eller att borrkärnsdatan varit begränsad.

Relevanta sökord: *brucit, Gåsgruvan, serpentinisering, dedolomitisering, skarn, 3D-modellering*

1 INTRODUCTION

1.1 Background and objectives

The Gåsgruvan quarry (Fig. 1) is located in the massive volcanogenic Bergslagen domain. SMA Mineral AB mines annually c. 225,000 tons of calcite marble within the Gåsgruvan open mine pit. The refined calcite marble is applied for various aims, such as construction work, concrete, agriculture and liming of lakes (SMA Mineral AB, 2018). The marble appears as coarse-grained crystals suitable for industrial use and shows low concentrations of accessory minerals (e.g. Lundegårdh, 1987). However, notable concentrations of the hydroxide mineral brucite [$Mg(OH)_2$] are present within the deposit. Brucite increases the pH of the flotation liquids which results in a worse yield of extracted marble. Black colored brucite may also reduce the whiteness of the product (Karlsen, 2000). A cooperative project between SMA Mineral AB and Gåsgruvan Kalcit AB (OMYA) has been established in order to research the interference of brucite.

The aim of this thesis was to localize all brucite-rich zones within the Gåsgruvan open mine pit through drill core mapping and complementary field mapping. Mapped brucite zones were correlated and the interpreted brucite distribution was demonstrated with a generalized 3D-model. Furthermore, the aim was to describe the local petrogenetic origin of brucite in various parts of the deposit, which was carried out with lithological drill core profiles and microscale studies. The hypothesis of this work was that brucite would follow a foreseeable pattern that could be visualized three-dimensionally. It was further assumed that the petrogenetic origin could be determined for the largest brucite zones. Some mapped zones could not be correlated nor associated with a single petrogenetic source due to the scattered nature of brucite.

1.2 Outline of the thesis

The first part of this thesis describes the geological setting of Gåsgruvan and the features of the study site. The characteristics and genesis of brucite are further presented. Material and methodology are presented in **the second part**. The results of brucite mapping, 3D-modelling, lithological profile interpretation and conducted micro-scale analysis are described. The geological environment and variations between occurring brucite are ultimately discussed.

Research questions:

- *How does the petrogenetic origin of brucite differ within the deposit?*
- *Can reliable correlations be made between mapped brucite mineralization zones or is the distribution too scattered?*
- *What are the field relations between brucite and the surrounding geology?*

Figure 1. Gåsgruvan open mine pit in August 2017. View towards southeast.

2 REGIONAL GEOLOGY

Gåsgruvan is located at the western margin of the Bergslagen region, in the south-western part of the Svecokarelian orogeny (Fig. 2) (Stephens et al., 2009) belonging to the Fennoscandian shield, which is composed of several accreted terranes. The northeastern part of the shield is composed of Archean rocks and the central part, i.e. the Svecokarelian orogen, comprise Palaeoproterozoic rocks (Lahtinen et al., 2005).

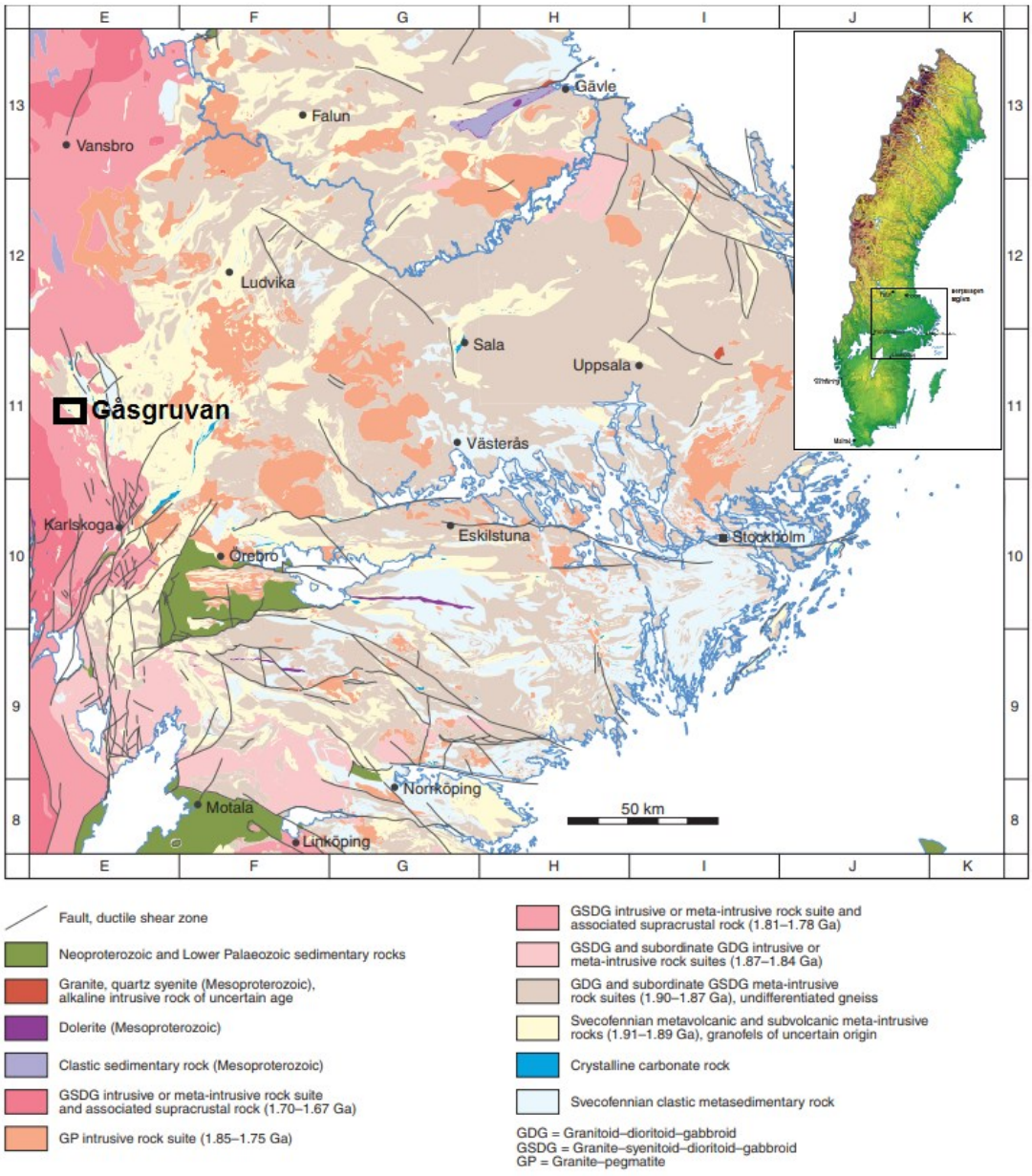

Figure 2. Simplified geological bedrock map of the Bergslagen region. The study site is highlighted with a black square. SGU Map, modified after Stephens et al. (2009).

The Svecokarelian rocks in Sweden were formed between 1.9 and 1.8 Ga (e.g. Allen et al., 1996, Stephens et al., 2009) with preceding arc magmatism between 1.95-1.9 Ga (Högdahl et al., 2004 and references therein).

2.1 Bergslagen region

The Bergslagen region is a felsic magmatic province formed in an extensional setting inboard an active continental margin (e.g. Allen et al., 1996; Stephens et al., 2009). Bergslagen, which is believed to be part of a back-arc environment, represents a mix of a terrestrial and marine caldera region built on continental crust (Allen et al., 1996). Ductile deformation occurred during several stages of both regional and contact metamorphism reaching greenschist to amphibolite facies. Granulite facies prevail locally in the southern part of the region (Stephens et al., 2009).

2.1.1 Early Svecokarelian rocks

The dolomitic and calcitic crystalline marble units of Bergslagen are deposited in a 1.9-1.88 Ga felsic, rhyolitic and/or dacitic metavolcanic succession (Fig. 3 & 4a). The felsic metavolcanic rocks are over- and underlain by metasedimentary rocks and conglomerates, such as metagraywacke, quartzite and meta-argillite (Stephens et al., 2009). Some metavolcanics occur also as intercalations in the metasedimentary rocks (Allen et al., 1996). The marble units are scattered throughout Bergslagen in minor occurrences, such as in Filipstad (Gåsgruvan), Sala and Vikern (Stephens et al., 2009). Some of these planar-bedded limestones are assumedly chemical sedimentary rocks whereas others may be stromatolitic limestones where the structures are either preserved or destroyed. Most chemical limestones are marine precipitates rather than exhalites of hydrothermal origin (Allen et al., 1996).

Regional subsidence and deposition of carbonate rocks and volcanic sandstone represent the upper part of the volcanic succession (Stephens et al., 2009). This succession hosts metallic mineral deposits such as iron oxides that may be high or low

in manganese and base metal sulphide deposits such as banded iron formations, magnetite-calc-silicate skarn mineralizations, carbonate-hosted and apatite-bearing iron ore and stratiform and strata-bound sulphide deposits (e.g. Allen et al., 1996).

Prior to the regional metamorphism, magnesium alteration (magnesium ± iron ± potassium ± silica) replaced feldspars by phyllosilicates in the metavolcanic rocks (Stephens et al., 2009). Mg-alteration has been explained through models of synvolcanic, regional and hydrothermal convection where hot seawater has circulated through glassy rocks. Ore-forming elements leached to lower volcanic successions, whereas Mg was enriched in the upper parts (Allen et al., 1996).

The Svecokarelian orogen was affected by Svecokarelian deformation and metamorphism at 1.85-1.8 Ga. The early orogenic rocks, including the volcanic and sedimentary rocks metamorphosed during two peak events (Stephens et al., 2009), with two associated rifting episodes (Beunk & Kuipers, 2012).

The early orogenic rocks were later intruded by felsic and mafic plutonic rocks of different generations (Stephens et al., 2009). Three NW-NNW striking, metamorphosed amphibolite dykes intrude the Gåsgruvan marble lens (Fig. 4b) (Lundegårdh, 1987). They show spilitic alteration and may have intruded during deposition of clastic sedimentary rocks (Stephens et al., 2009). The amphibolites overlay the marble horizon (Björk, 1986) and are associated with the felsic metavolcanics (Stephens et al., 2009). The metavolcanite sequence is intruded by albite-rich Horrsjö granite a few kilometers northwest of Gåsgruvan (Fig. 4c). This granite intrusion is part of the 1.89-1.88 Ga synvolcanic Horrsjö complex in the Långban-Nordmark area (e.g. Högdahl & Jonsson, 2004). The Horrsjö granite is tonalitic to alkali-feldspar granitic and shows geochemical similarities to the felsic metavolcanite. Horrsjö granite may have formed during volcanic activity and remobilized simultaneously with the metavolcanics during later folding (Åberg et al., 1983 and references therein).

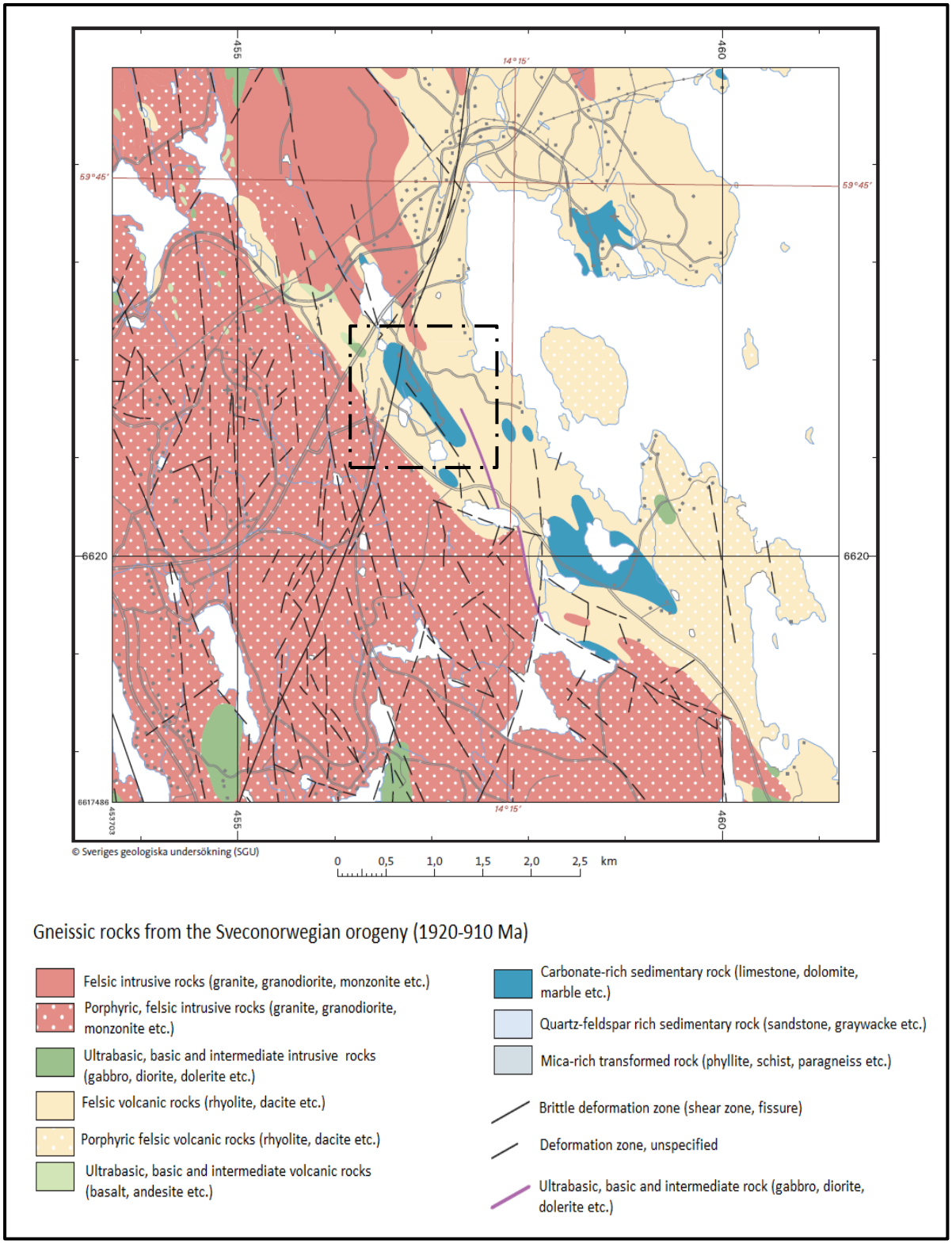

Figure 3. Site of study (*dashed square*) and local geological features (modified after the Geological Survey of Sweden, 2018).

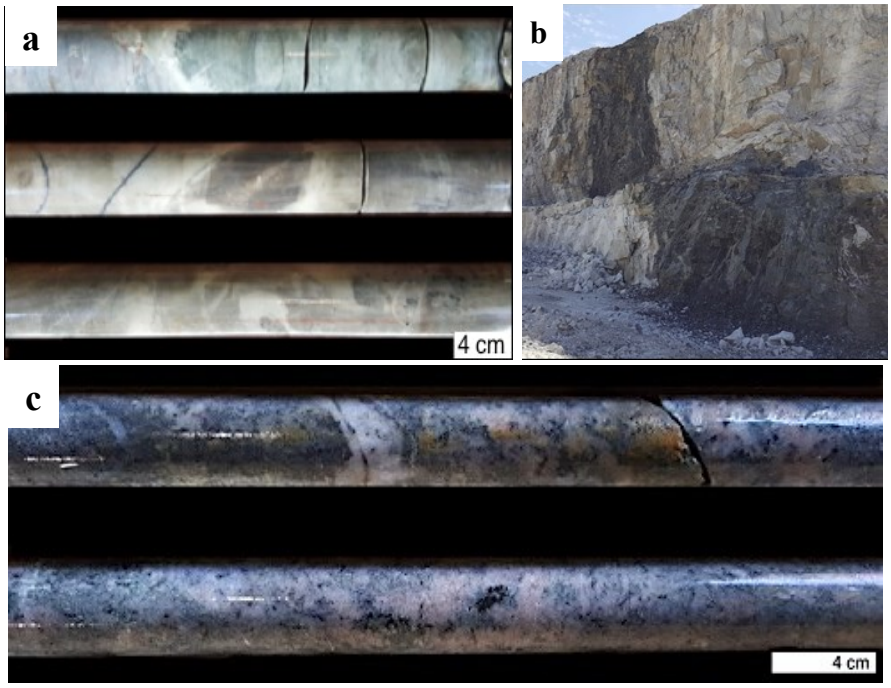

Figure 4. (a) Felsic metavolcanite from the southeastern part of Gåsgruvan. **(b)** A large amphibolite intrusion cuts the deposit at the western margin. Picture taken towards southwest. **(c)** Drill core sample of albite-rich Horrsjö granite from Gåsgruvan.

Mineral deposits of Bergslagen are often hosted in skarn (Allen et al., 1996; Stephens et al., 2009; Jansson & Allen, 2012). Skarn is the term for metasomatic Ca-Fe-Mg-(Mn)-silicate rocks that are formed through interaction between a carbonate and silicate systems (Bucher & Grapes, 2011). Skarn in Bergslagen was formed when calcareous, volcano-sedimentary rocks were affected by regional metamorphism. Skarn formed also during alteration by fluids from intrusions (Stephens et al., 2009). The strong metamorphic overprint has made it challenging to distinguish between the orogeny-related and the pre-regional metamorphism and intrusion-related skarn (e.g. Jansson & Allen, 2012).

Skarn in Gåsgruvan is defined as pyroxene- and garnet-rich skarn, and magnesian skarn (Fig. 5) (drill core data by SMA Mineral AB). Skarn is formed as a horizon around the deposit and as small lenses and veins within the deposit (Magnusson, 1925). Skarn that formed during greenschist-facies metamorphism is linked to mafic dykes (Stephens et al., 2009).

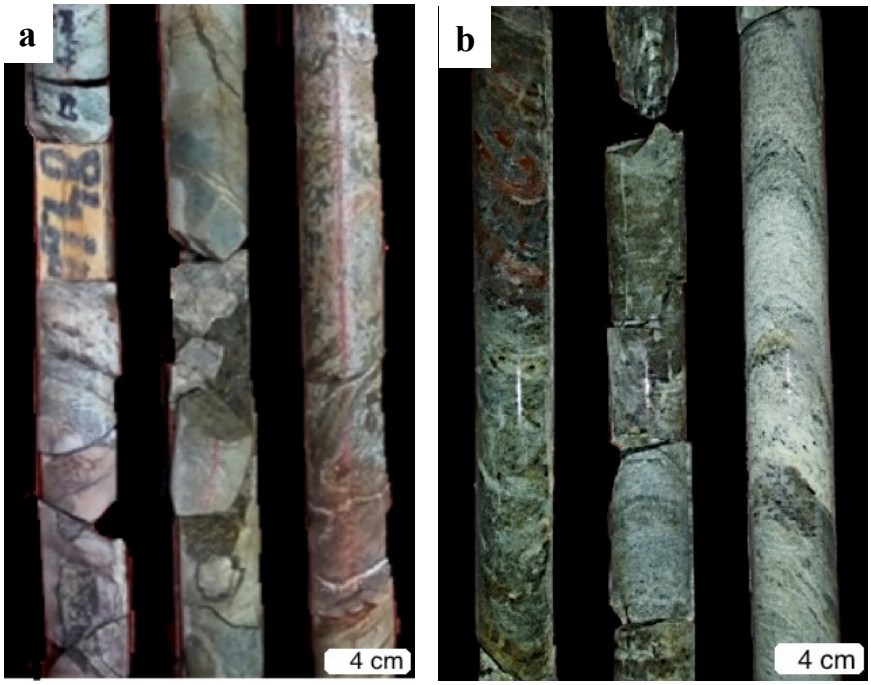

Figure 5. (a) Pyroxene skarn with flinty metavolcanite in Gåsgruvan (drill core 530). **(b)** Mg-altered skarn with chlorite and minor brucite in Gåsgruvan (drill core 510).

2.1.2 Rocks of the Transscandinavian Igneous Belt (TIB) and post-Svecokarelian intrusions

The western part of the Svecokarelian Domain is represented by the Transscandinavian Igneous Belt (TIB) (Högdahl et al., 2007). The TIB comprise 1.85-1.67 Ga intrusive and volcanic rocks (Gorbatschev, 2004; Stephens et al., 2009), further defined as large granitoid massifs and mafic intrusions. The plutonic TIB rocks are characterized by large feldspar megacrysts with massive and coarse matrix grains. The c. 1.8-1.78 Ga Filipstad suite belongs to the TIB (Högdahl et al., 2004) and margins the Bergslagen region to the west.

The southwestern border of Gåsgruvan comprise porphyric and TIB-related Filipstad granite (Högdahl et al., 2007). The 1783±10 Ma (Jarl & Johansson, 1988) Filipstad granite is part of the TIB-1 (1.81-1.76 Ga) granitic rocks within the Småland-Värmland Belt (Fig. 6) (Högdahl et al., 2004 and references therein). The composition

of Filipstad granite ranges from granitic to granodioritic. Some varieties can be quartz monzonitic and tonalitic (e.g. Högdahl et al., 2004).

Mafic and intermediate, co-magmatic rocks are found mingling and mixing with granitoids in the western Bergslagen region. Many of these mafic rocks are defined as large xenoliths of Svecokarelian metabasic rocks. The youngest TIB-related intrusions are represented by dolerite dykes of two generations (Högdahl et al., 2004 and references therein).

The western parts of Bergslagen were overprinted by Sveconorwegian deformation at 1.0-0.9 Ga (Stephens et al., 2009). A Sveconorwegian dolerite dyke intersects the bedrock northeast of Gåsgruvan (Sandström et al., 2009 and references therein).

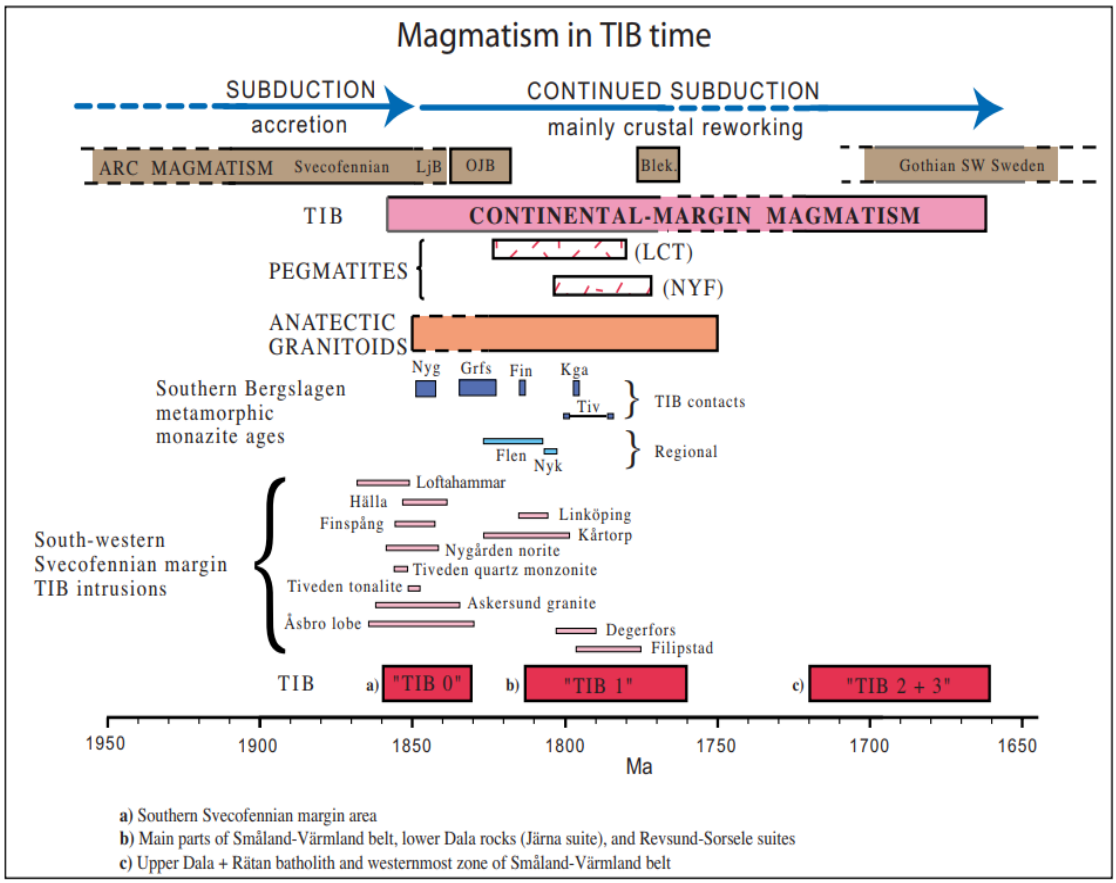

Figure 6. Definite timeline for the main plate-tectonic settings, and magmatic and metamorphic events in southern Bergslagen and the Småland-Värmland Belt. The 1.81-1.76 Ga Filipstad granite is part of the TIB 1 rocks (LjB = Ljusdal Batholith, Oskarshamn-Jönköping Belt, Blek = Blekinge Province) (Högdahl et al., 2004 and references therein).

3 SITE DESCRIPTION

The Gåsgruvan quarry is located four kilometers northeast of the Filipstad municipality in western Bergslagen (Shaikh et al., 1989). SMA Mineral AB mines calcite marble in Gåsgruvan in the open mine pit (Lundegårdh, 1987). The marble lens is approximately 1,400 meters long and 50-250 meters wide. Drill core data confirms that the marble body extends to a depth of c. 270 meters (Lundegårdh, 1987; drill core data of SMA Mineral AB).

The Gåsgruvan marble is massive or slightly foliated and white-greyish in color (OMYA, 2011). The marble is partially birefringent and medium to coarse-grained (Stuge, 1986; Lundegårdh 1987). The grains have a granoblastic texture with triple junctions of 120° (OMYA, 2014), which indicates deformation in a near-static stress regime (Winter, 2014). The marble lens strikes NW-NNW and the dip of the deposit varies between 60-75° SW and 70-80° NE, as recorded in drillings south of the present open mine pit (Stuge, 1986; Lundegårdh 1987).

The deposit is intersected by two north-south oriented shear zones. The shear zones margin the deposit in west and east. The contacts of the hanging wall and footwall are strongly fractured and filled with weathered talc-chlorite schist (Stuge, 1986; Lundegårdh 1987). This fractured, soil-like material is considered problematic, in addition to brucite, since it decreases the recovery and whiteness of the ore, and interferes with the floatation processes (OMYA, 2011).

76 minerals have been identified in Gåsgruvan and the most common ones are listed in *Table 1*.

Table 1. Commonly encountered minerals in Gåsgruvan (OMYA, 2011; Sandström et al., 2009). ***Identified in thin section (id), present with brucite (br).***

Mineral	Ideal formula	Identified (id)/present with brucite (br)
Annite	$KFe_3^{2+}AlSi_3O_{10}(OH,F)_2$	
Antigorite	$(Mg,Fe^{2+})_3Si_2O_5(OH)_4$	**id, br**
Brucite	$Mg(OH)_2$	**id**
Calcite	$CaCO_3$	**id, br**
Clinochlore	$(Mg,Fe^{2+})_5Al(AlSi_3O_{10})(OH)_8$	**id, br**
Clinochrysotile	$Mg_6Si_4O_{10}(OH)_8$	
Diopside	$CaMgSi_2O_6$	**id, br**
Dolomite	$(Ca,Mg)(CO_3)_2$	**id, br**
Fayalite/Forsterite	$(Mg_2^{2+}, Fe^{2+})_2SiO_4$	**br**
Fluorite	CaF_2	
Goethite	$FeO(OH)$	
Hedenbergite	$CaFe^{2+}Si_2O_6$	
Hematite	Fe_2O_3	
Magnetite	Fe_3O_4	**id, br**
Meionite	$Ca_4Al_6Si_6O_{24}CO_3$	
Microcline	$KAlSi_3O_8$	
Muscovite	$KAl_2(Si_3Al)O_{10}(OH,F)_2$	
Phlogopite	$KMg_3Si_3AlO_{10}(F,OH)_2$	**id, br**
Plagioclase	$NaAlSi_3O_8$-$CaAl_2Si_3O_8$	**id**
Pyrite	FeS_2	**br**
Pyroaurite	$Mg_6Fe_2^{3+}(CO_3)(OH)_{16}{\cdot}4H_2O$	
Pyrrhotite	$Fe_{1-x}S$	
Quartz	SiO_2	**br**
Spinel	$MgAl_2O_4$	**id, br**
Sphalerite	$CuFeS_2$	
Talc	$Mg_3Si_4O_{10}(OH)_2$	**br**
Tremolite	$Ca_2Mg_5Si_8O_{22}(OH,F)_2$	
Wollastonite	$CaSiO_3$	**br**

4 BRUCITE

4.1 Characteristics and appearance

Brucite is a hydroxide mineral that belongs to the hexagonal crystal system and has the formula of [$Mg(OH)_2$] (Mottana et al., 1983). Brucite can be transparent, green, blue or grey, and manganese-rich varieties (substitution of Mn^{2+} for Mg) are deep brown or brownish red. Brucite has a hardness of 2.5 and appears in foliated, scaly or

finely granular masses (Anthony et al., 2001-2005). Brucite occurs mainly in Italy, Sweden, USA and in asbestos in Canada (Schumann, 1992). Brucite is stable in rocks that are absent with SiO_2 since these minerals cannot maintain their own CO_2-rich fluid phase (Bucher & Grapes, 2011).

Brucite is a moderately appearing mineral in the Bergslagen region. It is mainly documented in the Värmland region (Fig. 7) but also in large sulphide deposits in east (Anthony et al., 2001-2005). Geochemical analysis revealed that brucite contains >14% Mn, hence being named manganese-brucite.

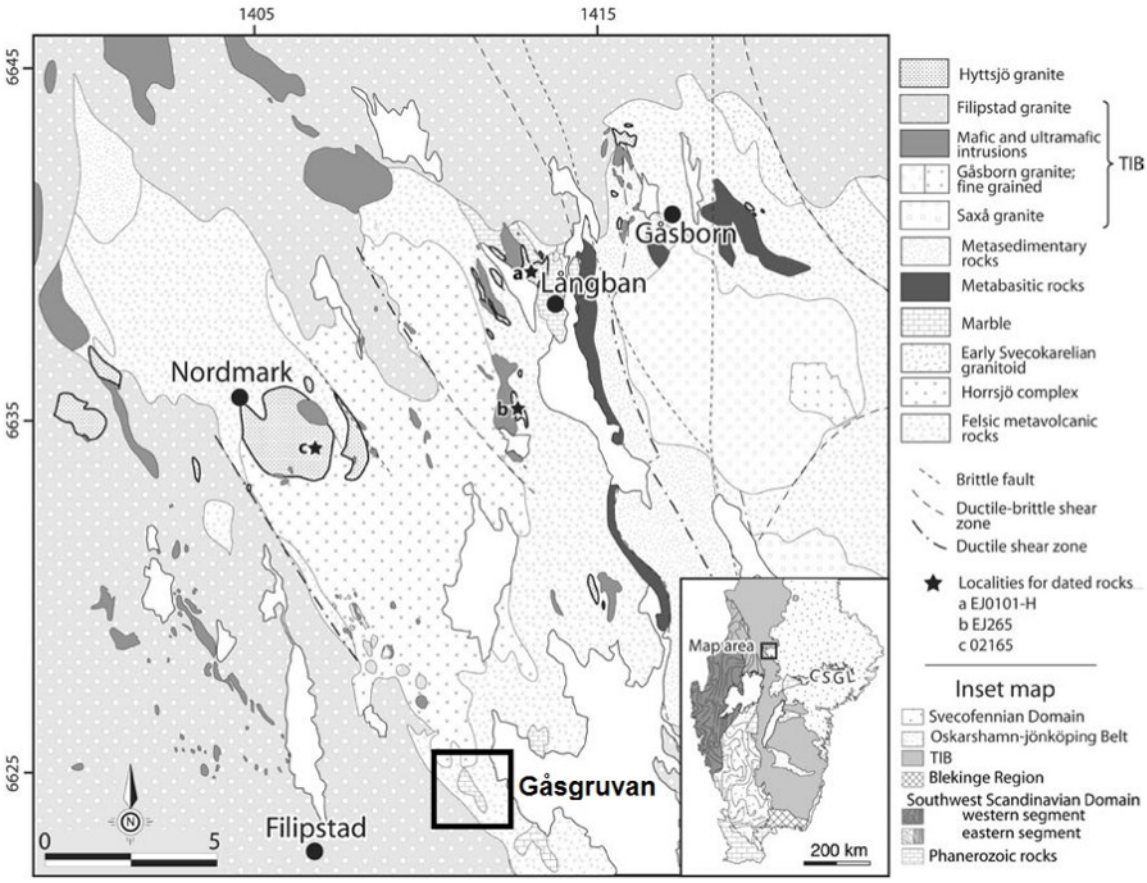

Figure 7. Brucite occurs extensively in Värmland, in e.g. Gåsgruvan, Långban and Nordmark (map after Högdahl et al., 2007).

In Gåsgruvan, the dolomite marble in the eastern hanging wall is brown and brucite-enriched (Stuge, 1986; Lundegårdh 1987). Brucite appears as transparent and brown grains (Fig. 8) and is associated with younger eruptive intrusions (Magnusson, 1925). The average CaO/MgO_{carb} ratio of the brucite marble is 1.66 (CaO = 35.8; MgO = 21.63) (Magnusson, 1925) corresponding to a dolomitic composition (classification

after Pekkala, 1985). Whole-rock analysis of brucite-rich dolomite marble in Gåsgruvan shows MgO concentrations of c. 20 % (Lundegårdh, 1987).

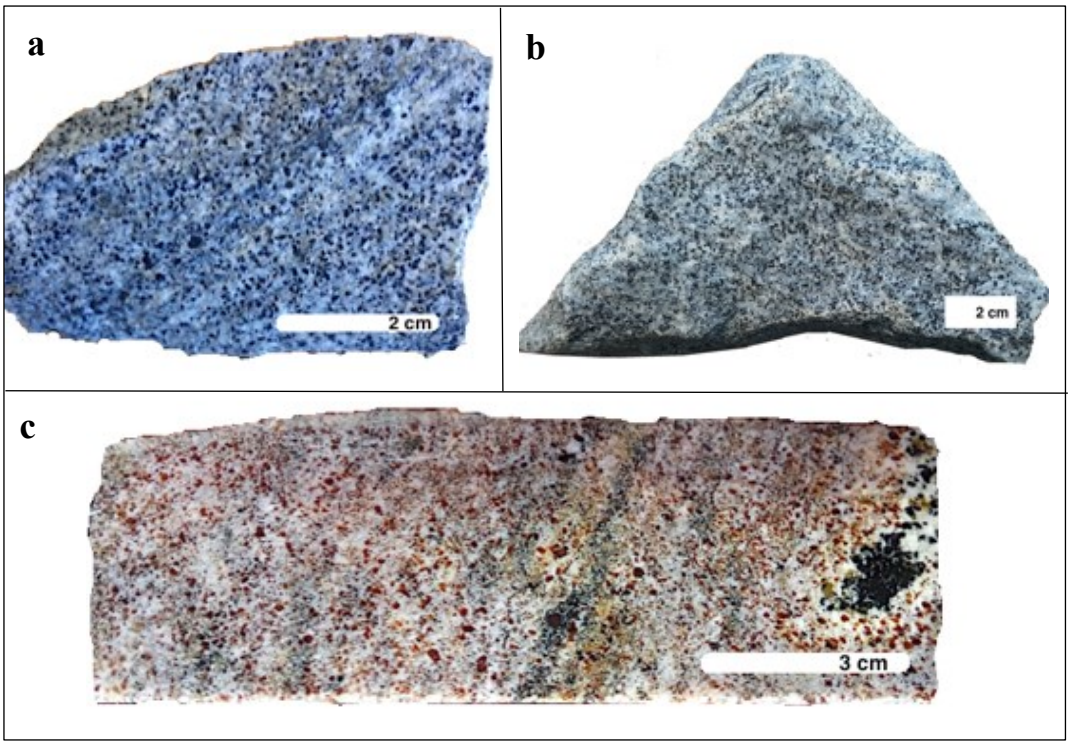

Figure 8. Brucite specimens, sampled at Gåsgruvan. **(a)** Light grey, moderate-sized brucite in dolomite marble. Sampled from the southeastern mining pit. **(b)** Brucite marble, sampled from northwest. **(c)** Brown-red, manganese-rich variety of brucite, sample of drill core series 600.

4.2 Genesis of brucite

Brucite is a metamorphic mineral and is found in carbonate rocks in low-temperature hydrothermal veins where thermal waters could percolate through the carbonate. It is also found in chlorite schists, talc schists and low-temperature serpentinized rocks (Mottana et al., 1983). Magnusson (1925) implied that brucite of Gåsgruvan is formed by contact metamorphism of dolomite. Analyses conducted by Wennerström (2015) and OMYA (2014) have further assessed that brucite in Gåsgruvan is related with Mg-rich hydrothermal fluids and contact metamorphism between the marble and locally heated igneous intrusions. At the moment, two main hypotheses of brucite formation have been suggested, namely dedolomitization and serpentinization.

4.2.1 Dedolomitization

Brucite is formed by isochemical contact metamorphism between dolomite and an igneous source. Dolomite decomposes by dissociation of the magnesite component, whereas the calcite component remains stable. Dolomite loses half of its CO_2-component (Bucher & Grapes, 2011) and if CO_2 is mobile, periclase (MgO) is formed (Reaction I) (Magnusson, 1925; Turner, 1965). Brucite is formed during the last metamorphic stage by retrograde hydration (Bucher & Grapes, 2011) (Reaction II). Brucite in Gåsgruvan resembles the mineral predazzite (Magnusson, 1925) where periclase has either been transformed to retrograde hydromagnesite or brucite (Turner, 1965).

$$\underset{\text{Dolomite}}{CaMg(CO_3)_2} \rightleftarrows \underset{\text{Calcite}}{CaCO_3} + \underset{\text{Periclase}}{MgO} + CO_2 \qquad \textit{(Dedolomitization, reaction I)}$$

$$\underset{\text{Periclase}}{MgO} + H_2O \rightleftarrows \underset{\text{Brucite}}{Mg(OH)_2} \qquad \textit{(Hydration, reaction II)}$$

(e.g. Watanabe, 1935; Müller et al., 2009)

A T-X_{CO2} diagram with a 1 kbar isobaric constant shows that brucite is formed at T = ≤600°C with absent CO_2 (Fig. 9), which also corresponds to an isobaric constant of 2 kbar (Bucher & Grapes, 2011).

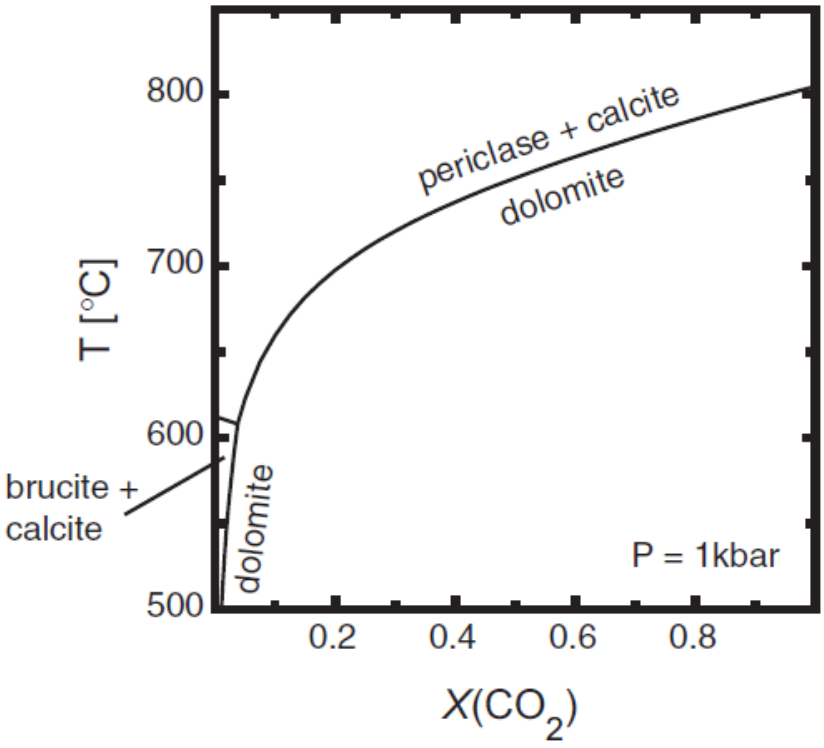

Figure 9. Brucite is formed at T≤600°C, close to absent CO_2, with an isobaric pressure (P) constant of 1 kbar (Müller et al., 2009).

4.2.2 Serpentinization

When an anhydrous forsterite (Mg-rich olivine) is hydrated, retrograde serpentine, ±brucite (and ±magnetite) are formed at ≤500°C during a serpentinization event (Fig. 10, Reaction III). Serpentinization occurs in oceanic ophiolite complexes, in the mantle and in the crust during collision belt formation (Bucher & Grapes, 2011). The iron-rich fayalite-component of olivine may enter the structure of serpentine or brucite or form separate phases such as magnetite or ferrite-chromite (Ashley 1975; Moody 1976).

$$\underset{\text{Forsterite}}{(Mg_{1.8}, Fe_{0.2})SiO_4} + 1.37H_2O \rightleftarrows \underset{\text{Serpentine}}{0.5Mg_3Si_2O_5(OH)_4}$$

$$+ \underset{\text{Brucite}}{0.3Mg(OH)_2} + \underset{\text{Magnetite}}{0.067Fe_3O_4} + 0.67H_2 \qquad \text{(reaction III)}$$

(Huang et al., 2017)

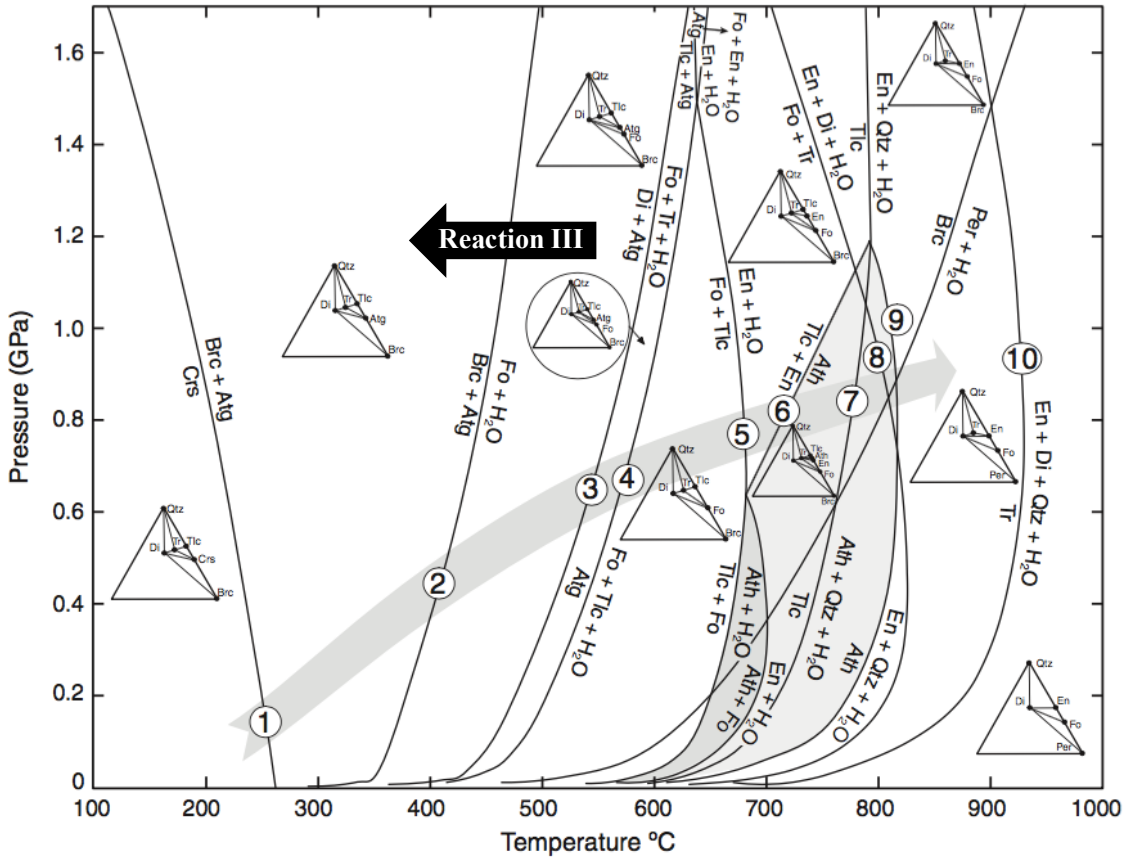

Figure 10. Petrogenetic grid for H_2O-saturated ultramafic rocks in the CaO-MgO-SiO_2-H_2O system. Serpentinization of forsterite forms retrograde antigorite and brucite at c. 350–450 °C (Winter, 2014). (Atg = antigorite, Brc = brucite, Fo = forsterite)

5 MATERIAL AND METHODOLOGY

5.1 Sampling and thin section preparation

A total of nineteen thin sections were examined in this thesis. Fifteen thin sections of brucite marble, partly altered marble and skarn breccia were prepared at the laboratory of Åbo Akademi University and Turku University. The samples were selected from brucite rich environments within the open mine pit. Five samples from the field, seven drill core samples from series 500 and two drill core samples from series 600 were hand-picked. The thin sections were polished to a thickness of 30 µm and placed on a glass slide with epoxy. Complementary thin sections were provided by SMA Mineral

AB. However, only four of these thin sections showed considerable amounts of brucite for further analysis. Petrographic analysis and photogrammetry were conducted with a Leica polarized light microscope, with the objectives 2.5/0.08, 6.3/0.2 and 10/0.25 at the microscopic laboratory of Åbo Akademi University.

Sample DC500.11 represents skarn breccia with some titanium-rich ilmenite. Sample DC534.4 contains calc-silica minerals such as chlorite, diopside and forsterite with no brucite. Wennerström (2015) associated the appearance of titanium with forsterite breakdown and chlorite with chloritization of forsterite. These samples are not further discussed in this thesis.

5.2 SEM-EDS

Micro-scale analysis was further conducted with Scanning Electron Microscopy with an energy-dispersive X-ray spectrometer (SEM-EDS) at TopAnalytica, operated by Casimir Näsi. A JEOL IT-100 InTouchScope Scanning Electron Microscope with an EDS detector JEOL DPP5 was used. Samples FS*15*, FS*25*, DC*503/13*, DC*515/65, DC500/11* and *DC528/13a* were analyzed in order to identify mineral assemblages that could not be determined with optical microscopy. In order to shorten the analysis run, low-vacuum mode was used. No pre-treatment was required even if the samples were non-conductive (Jeol, 2018). The assessment of results was constrained, since low-vacuum mode is only semi-quantitative. In addition, the key hydroxide groups of e.g. serpentine and brucite were not possible to analyze due to the nature of EDS analysis. To determine the minerals, the results were compared to reference values.

5.3 Drill core mapping

The Gåsgruvan Access database is comprised of collar data from drill core series 500, 600 and 014. All prevailing drill cores were relogged during the summer and autumn

of 2017 by the author. Series 014 was not examined further since the data would have been too extensive to analyze during this study.

The relogging was carried out with the aim to estimate the quantity of brucite in each core interval by utilizing a percentage chart of Terry & Chilingar (1955). A simplified classification system with five categories was developed in order to facilitate the estimation (Table 2).

Table 2. **Simplified classification of estimated brucite content.**

Green	No abundant brucite, trace amounts of chlorite or magnetite may appear.
Yellow ***(BRCM)***	3-5% brucite, evenly distributed and fine to moderately sized black/transparent grains.
Orange ***(BRCM)***	Moderate (10-20%) brucite concentrations. Grains are mainly gray-transparent/black, red-brownish or black depending on substituted Fe and Mn. Magnetite is identified with a handheld magnet.
Red ***(BRCH)***	Brucite marble with c. 40-60% brucite.
Dark red ***(BRCH)***	Red-brown brucite and/or black with varying grain sizes. At least 70% brucite.

Drill core series 500 and 600 comprise altogether approximately 7900 m of diamond drilled material and are drilled in cross sections with internal spacing of 50 meters. Each cross section contains 1-3 drill cores (OMYA, 2011). The drill cores are drilled linearly, and the lengths vary between 5.4-296.8 meters.

Lithological profiles of drill cores 503, 504, 507, 515, 518 were provided by SMA Mineral AB. The profiles were modified with the GIS-software QGIS™ in order to understand the relation between brucite and associated lithological units. Drill core 504 is drilled close to drill core 507 in the eastern deposit. Drill core 503 is drilled in east, outside the active mining area. Drill cores 515 and 518 are drilled in the central deposit.

Drill cores 605, 606, 627 and 628 are examined briefly in this thesis due to the high brucite abundance. Drill cores 605 and 606 are drilled in the western deposit, whereas drill cores 627 and 628 are drilled deep in the central quarry and share the same location but differ in orientation.

5.4 Field mapping

Complementary field mapping of brucite was carried out within the open mine pit with a Trimble© Geo7X handheld data collector equipped with a GNSS Zephyr satellite-antenna. The quarry was divided into nine geographical sites (Fig. 11) that differed petrologically. Coordinates from this field mapping were inserted in the final 3D-model.

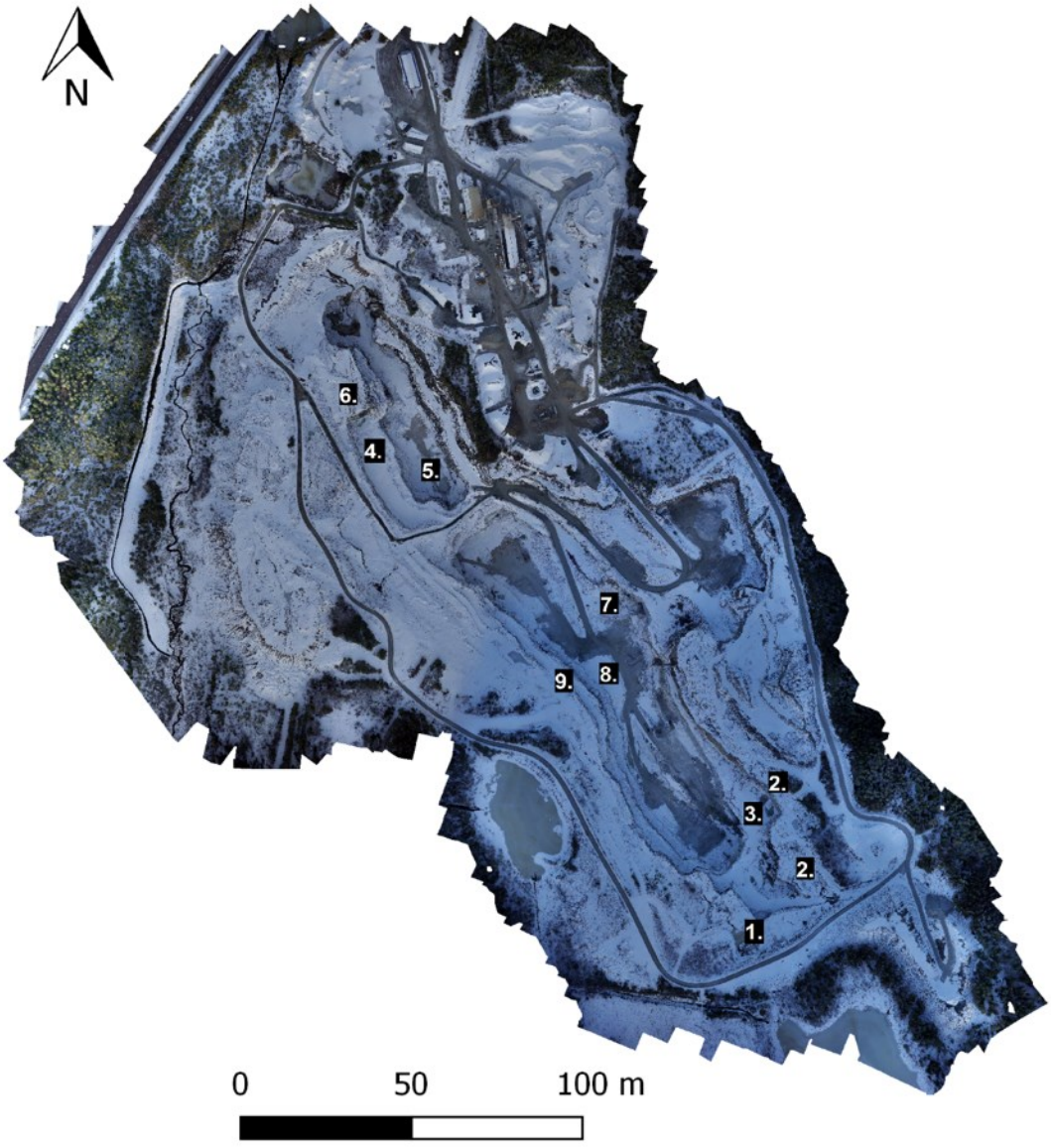

Figure 11. The Gåsgruvan quarry and mapped field sites 1-9 (orthophoto winter 2017, modified after SMA Mineral AB).

5.5 3D-modelling

The 3D-modelling was conducted with Dassault Systèmes'® geological and resource modeling software GEOVIA Surpac™ in order to demonstrate and examine the correlated brucite zones.

A Microsoft Access database was created for the raw data. The visualized drill cores comprised a compulsory collar and survey table, and an optional geology and assay table. The brucite modelling was composed with the following parameters: Drill core data with an XRF-analyzed ratio of $MgO/SiO_2 \geq 1$ and core mapped moderate (>10%, <40%) and high quantity (>40%) brucite zones. The coordinates from field mapping were also utilized (Fig. 12). The ratio between MgO and SiO_2 enhances Mg-rich minerals such as brucite, and eliminates silica-rich minerals such as forsterite, phlogopite, serpentine and talc. High MgO/SiO_2 zones and core mapped brucite zones corresponded well which facilitated the modelling (Fig. 13). Logged brucite data from disposed drill cores were disregarded.

All core logged data from series 500 and 600, and field mapped data were inserted in the software within the Sweref 99 1330 coordinate system. The displayed core intervals were sectioned with the tool "graphically defined areas" and digitized into larger units. Each section was extruded and triangulated into a 3D-solid. The solid was colored yellow or red depending on the brucite concentration. Each solid was copied 1-2 meters perpendicular to the segment plane to form a larger brucite-rich unit. Ultimately all smaller 3D-solids/segments of correlated brucite zones were triangulated into larger units.

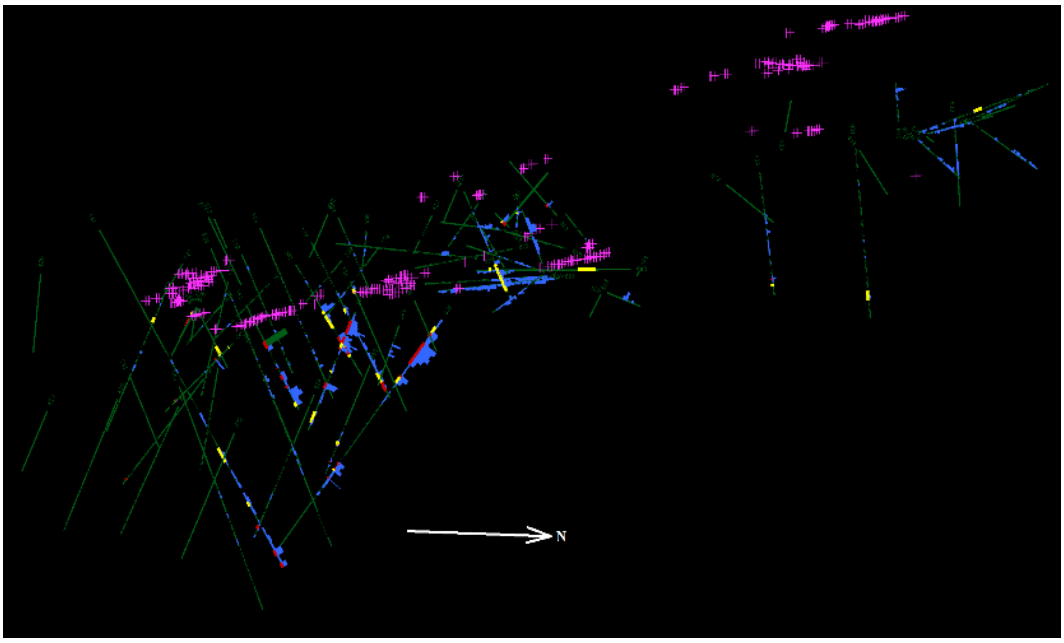

Figure 12. Core mapped brucite-rich zones (yellow and red), field mapped brucite (purple) and zones where XRF-data shows MgO/SiO_2 ratios ≥1 (blue bar) were used as parameters for 3D-modelling. Some overlapping XRF-values are displayed with green bars. Viewed from east.

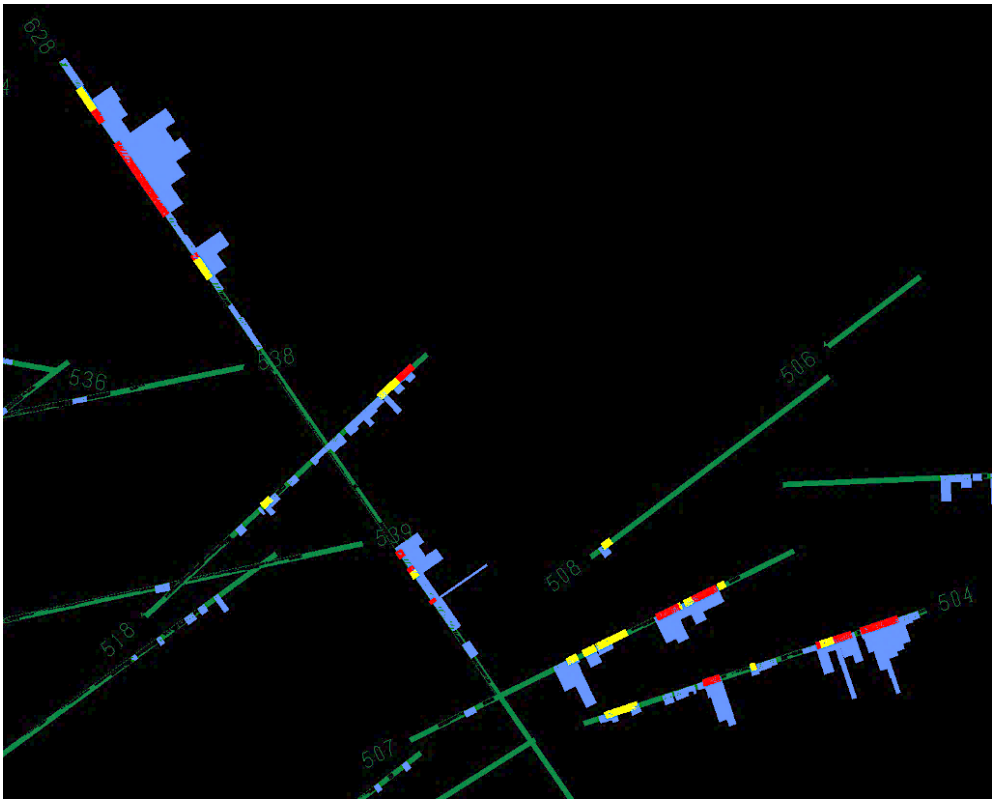

Figure 13. The MgO/SiO_2 ratio (blue bar) corresponds well with core mapped brucite (yellow and red). The highest anomalies are present in drill core 507, 504 (lower right) and 628 (upper left). Viewed towards north.

6 RESULTS

6.1 Field site mapping

Most brucite in Gåsgruvan was found in field site 1 (south), 2 (southeast-east), 4 (northwest) and 9 (west). The results of microscale analysis in these field sites are discussed later and the sampling coordinates are presented in Appendix B.

6.1.1 Field site 1-3 – southern, southeastern quarry

Brucite in *field site 1* is characterized by incoherent, sporadic brucite mineralization in contamined marble. The marble hosts some felsic metavolcanite intercalations (Fig. 14a) and minor sulphide and oxide minerals. Antigorite is present with brucite (±magnetite) (Fig. 14b). Most brucite veins strike uniformly 325-350°N (Table 3-1) and continue towards north. Some brucite veins are branched from the same source southwards of the field site.

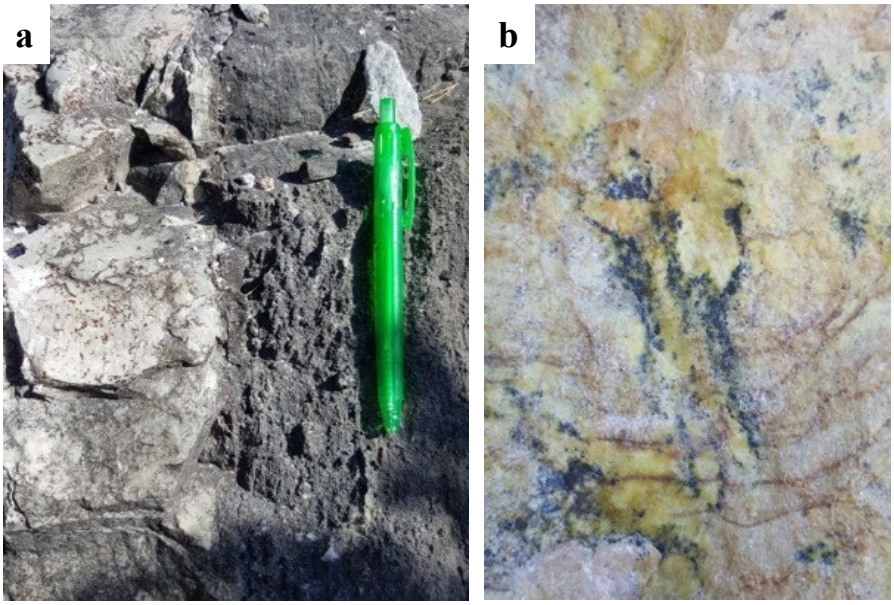

Figure 14. (a) Contact between a felsic metavolcanic sequence and darkened marble. The reference pen is c. 15 cm. **(b)** Antigorite, brucite and magnetite (?) in mineralized marble. The section view is c. 60 cm, view towards south (compare with field site 1; Figure 11).

The densest brucite zones occur at *field site 2*. Brucite is formed in the contact of mineralized amphibolite and dolomitic marble (Fig. 15). This large zone, with >50% brucite, extends coherently along the eastern margin and minor antigorite is also found.

Brucite in *field site 3* appears as rapid intercalations and is assumedly formed by dedolomitization where fluids have percolated through the marble. Some brucite may be associated with field site 2. Measured brucite strikes 340°N and the dip is near-vertical, corresponding to the marble foliation orientation.

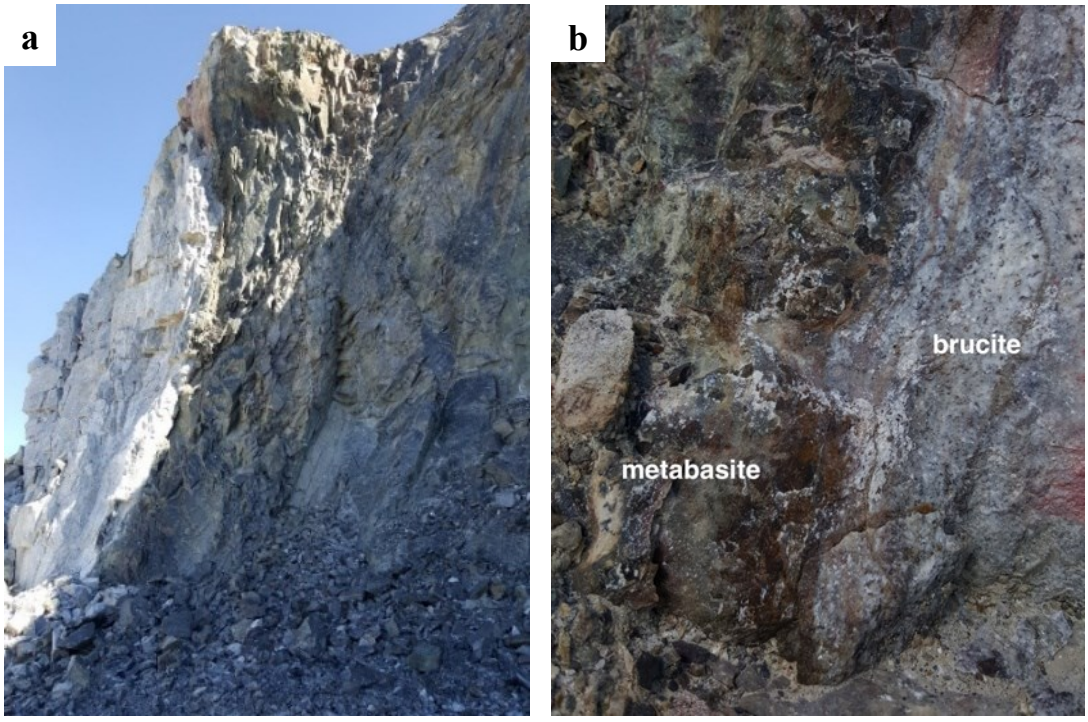

Figure 15. (a) Mineralized amphibolite dyke with e.g. chlorite schist. Viewed towards north from field site 3. **(b)** Brucite marble is found in the contact of mineralized amphibolite, field site 2.

Table 3-1. Description of mapped brucite mineralization in field sites 1-3.

GPS-ID	DESCRIPTION
11; 12	30-40% brucite, parallel veins.
15; 16	Thick brucite veins, strike 325-350°N. *Sample FS15.*
1.3; 1.5	Brucite in contact of mafic and felsic metavolcanite.
21-25	Massive brucite mineralization, mafic intrusion contact. *Sample FS25.*
31; 32	Thin veins of brucite, intervening incoherently.
33	Brown brucite grains near pit wall, strike approx. 340°N.

6.1.2 Field site 4-6 - northern quarry

Brucite is only abundant in the contact of the north-south intruding amphibolite in *field site 4* (Fig. 16). All brucite zones are oriented in the same direction as the amphibolite intrusion.

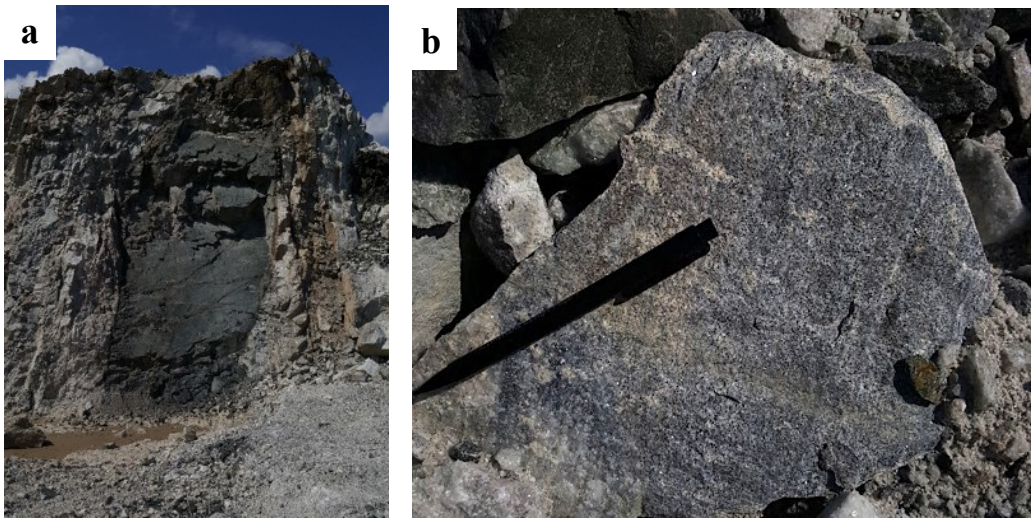

Figure 16. (a) Brucite is concentrated in the contact of intruding amphibolite. All brucite zones continue towards north. Viewed towards northwest. **(b)** Mined brucite-rich boulder close to the amphibolite contact.

Field site 5 is not discussed further since brucite appears scarcely in this area. The marble deposit at *field site 6* is cut by thick and long brucite zones which strike approximately 345°W. These brucite zones origin from site 4 and the brucite content is approximately 30-80%.

Table 3-2. Description of mapped brucite mineralization in field sites 4-6.

GPS-ID	DESCRIPTION
41;42	Parallel with amphibolite, 30-40% brucite.
61;63	Discontinuous brucite veins, two intervening veins.
62	Long vein, next to a mafic contact.
65-68	Massive brucite veins, continuing towards the precipice.

6.1.3 Field site 7-9 - central quarry

Field sites 7 and 8 are situated in the lowest part of the open mine pit where brucite is located on both sides of the pit wall. Field site 8 represents the most active mining area today but here brucite appears in scattered zones without any foreseeable pattern and an unknown origin. *Field site 9* represents a rapid sequence of brucite in immediate contact of skarn (Fig. 17a) and iron oxides (Fig. 17b). The brucite marble is oxidized and brown (Fig. 17c).

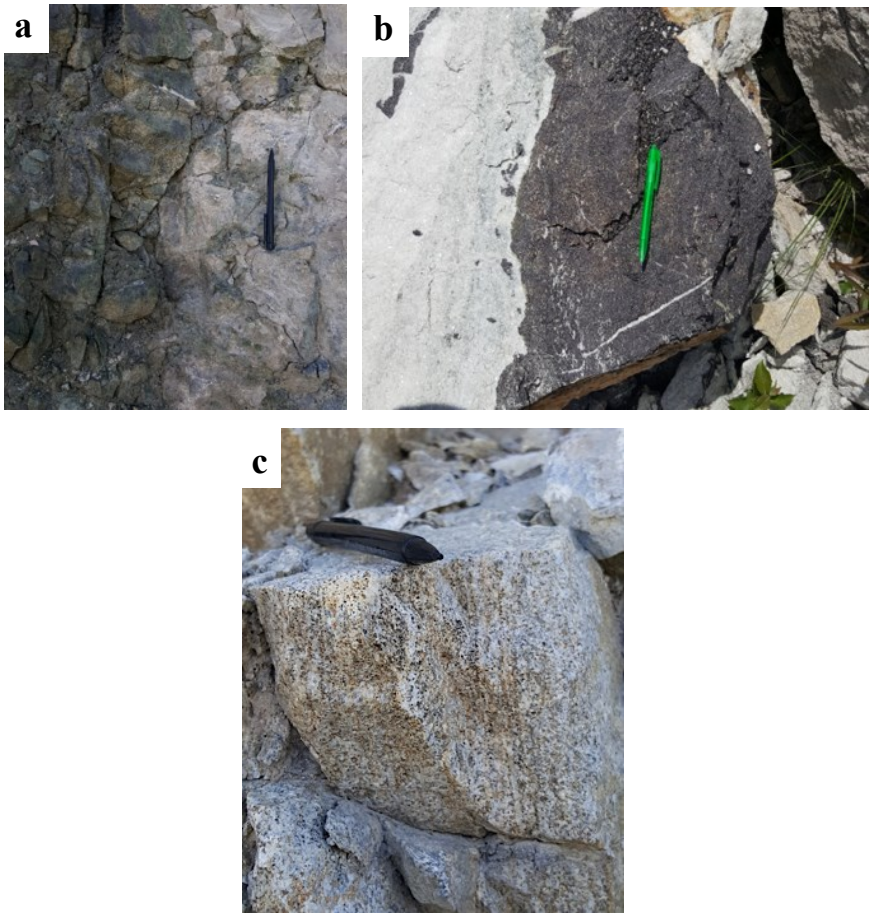

Figure 17. (a, b) Epidote- and pyroxene-rich skarn is abundant with some iron oxides in the proximity of brucite. **(c)** Rapid mineralization zone of brucite-rich and oxidized marble. View towards west.

Table 3-3. Description of mapped brucite mineralization in field sites 7-9.

GPS-ID	DESCRIPTION
71	Thick brucite sequence, 70° dip towards W.
73;74	Vertical brucite veins, strongly visible.
77;78	Moderately visible, 20% brucite.
79	Very mineralized brucite vein, 40% brucite.
92A-C	Highly mineralized brucite zone near iron oxides and skarn.

6.2 3D-modelling results and interpretations

All correlated and demonstrated brucite zones are based on bold interpretations and function as a guideline for the general distribution of brucite. This interpretation is shown with moderate and high quantity brucite zones (Fig. 18), and is divided into southern, central and northern deposits.

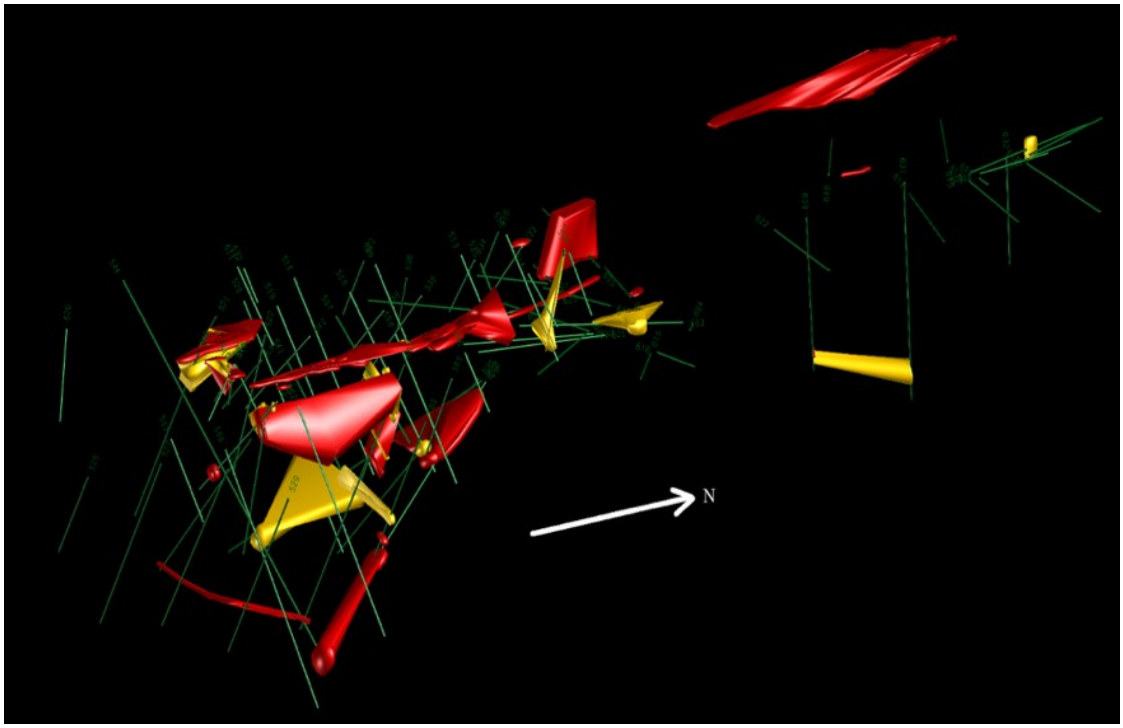

Figure 18. Bold interpretation of brucite distribution in the Gåsgruvan quarry. Red zones = high quantities (>40%) of brucite, yellow zones = moderate quantities (c. 10-40%) of brucite.

Brucite is mainly abundant in the southern and southeastern part of the quarry in a crescent structure that follows the outlines of field mapped sites 1 and 2 (Fig. 19a). Brucite in the field site 1 and 2 is interpreted using GPS-mapped coordinates. The southern mineralization zone extends deep into the deposit, especially at the field site 2. Brucite occurs southward of this large crescent zone, deep in some drill cores from series 500. Brucite does not appear near the surface, despite amphibolite and skarn being present here.

Brucite is abundant as two separate units deep in the south-central part of Gåsgruvan. One of these units contains high quantities of brucite and may form a continuum towards north. The other south-central unit, which is located southward of the first unit, comprises moderate quantities of brucite. This unit is separate from all other modelled brucite zones.

In the central and northern part, brucite appears as scattered intercalations (Fig. 19b). In the northern deposit, brucite follows the contact of a large amphibolite intrusion that margins the deposit in the west. The brucite zone described in field site 4 and 6 is correlated with brucite deep in drill cores 630 and 631. Interpretations of correlated brucite zones are difficult to determine here due to limited data. Correlations are mainly based on inserted GPS-coordinates of field mapped brucite.

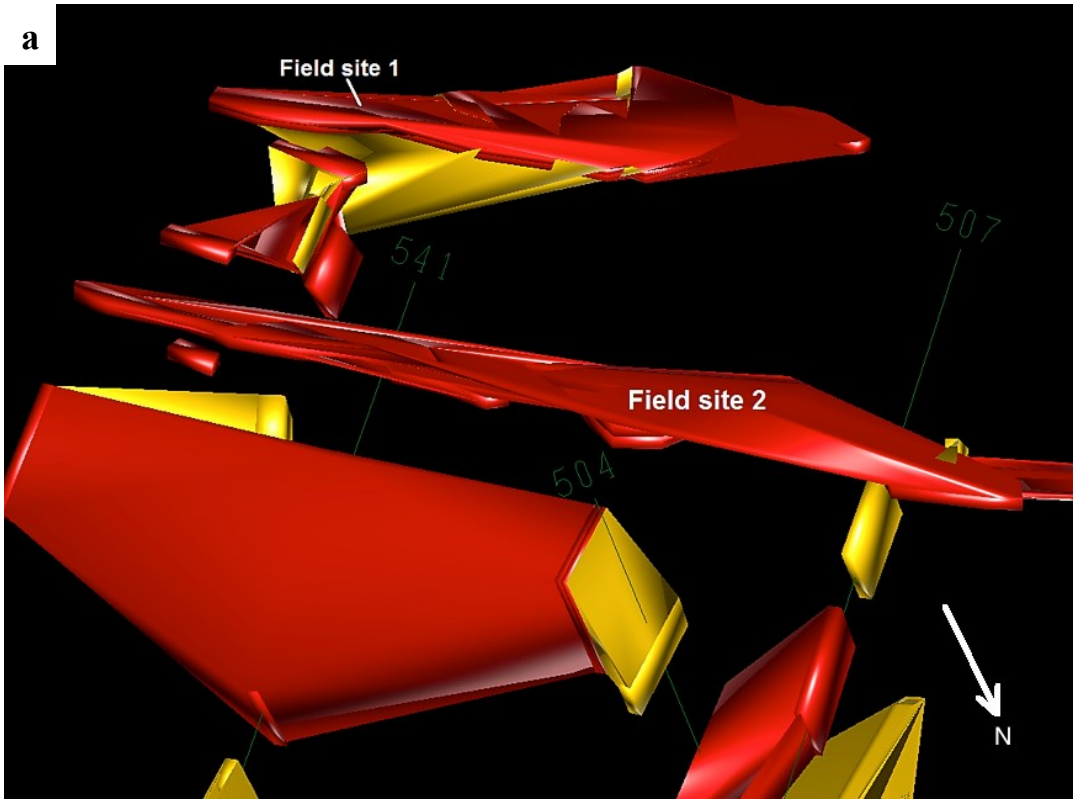

Figure 19. (a) Field site 1 and 2 form a crescent structure of brucite in the southern part of the deposit. Brucite in field site 2 is correlated with interpreted brucite-rich zones in drill cores 504, 507 and 541. Viewed towards southwest.

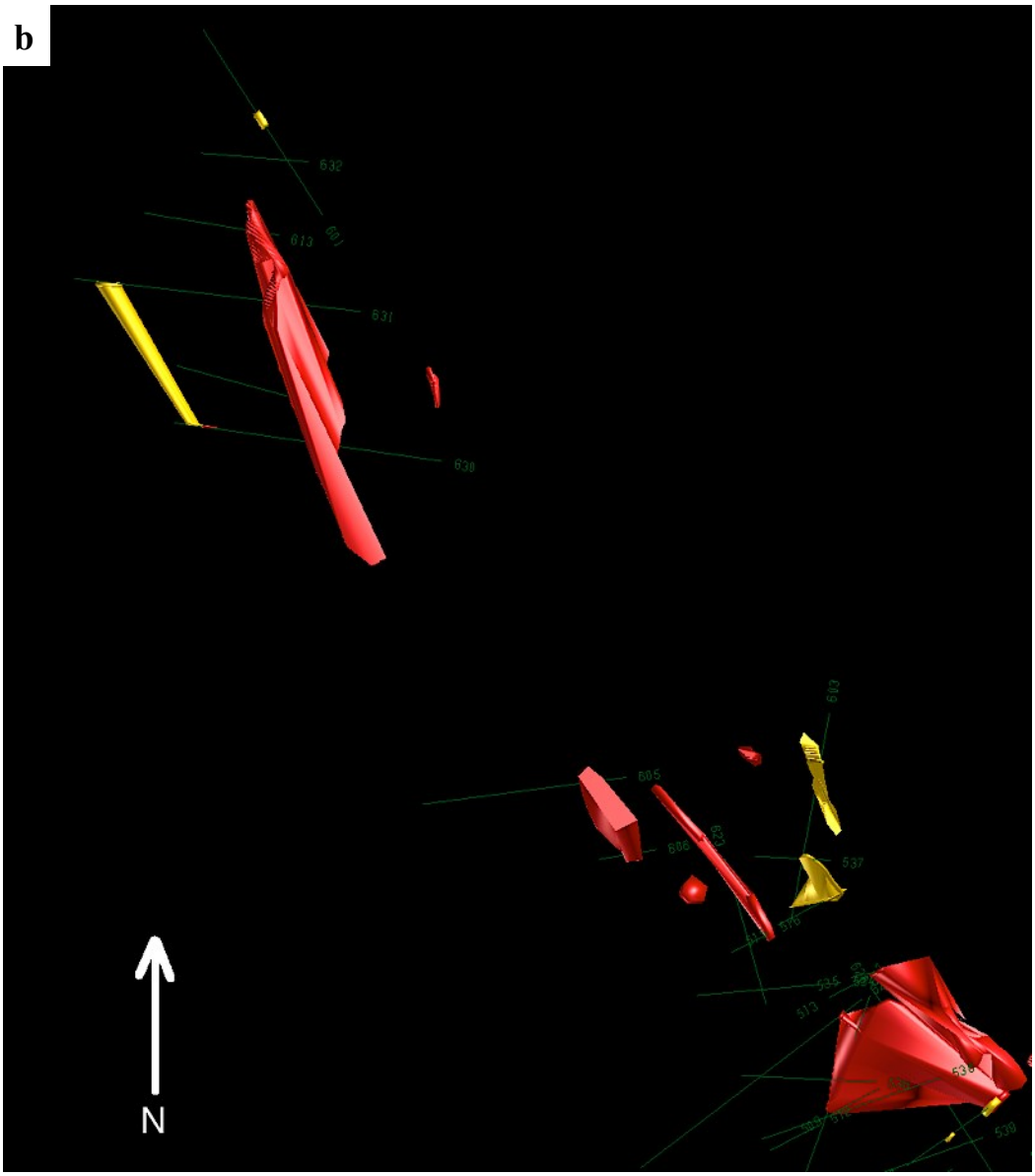

Figure 19. (b) The distribution of brucite is scattered in the central and northwestern deposit. Some correlations were found between GPS-mapped brucite zones. Zones in northeast were not modelled since all drill cores are disposed and the core data was therefore considered unreliable. Viewed from above.

6.2.1 Relation to mafic intrusions

The interpreted brucite zones are demonstrated together with the general features of post-peak metamorphic amphibolite intrusions (blue) and a 1.0-0.9 Ga dolerite dyke (purple) (Fig. 20). The younger dolerite dyke intrudes Gåsgruvan in southeast, whereas large amphibolite intrusions appear along the western and southeastern margin. Some

amphibolites were found as sporadic intercalations in the marble but these were considered too complex to model in this thesis.

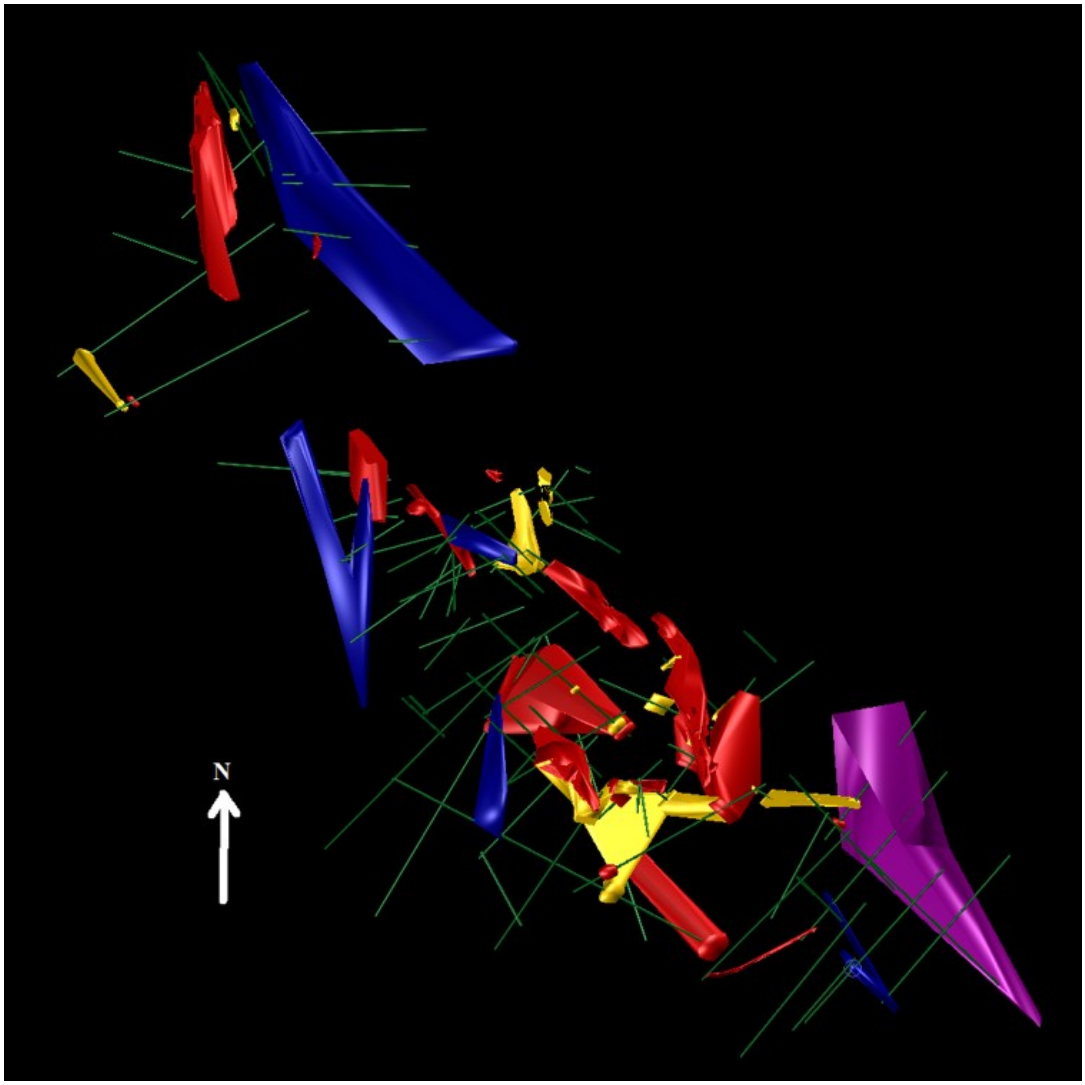

Figure 20. Modelled brucite zones in relation to the main features of the dolerite dyke (purple) and older, post-peak metamorphic amphibolite (blue). The colors of brucite are displayed in accordance with figure 16.

6.3 Drill core results

6.3.1 Cross section profiles of series 500

According to the lithological profile of drill core 503, brucite is mineralized in marble between a younger Sveconorwegian dolerite dyke and a narrow amphibolite intrusion (Fig. 21; compare with Fig. 20). Brucite may originate from both mafic sources but is assumedly related with amphibolite. Brucite does not appear in the direct igneous contact, but rather scattered within the marble. The mineralization zone is interpreted to continue vertically along the illustrated profile.

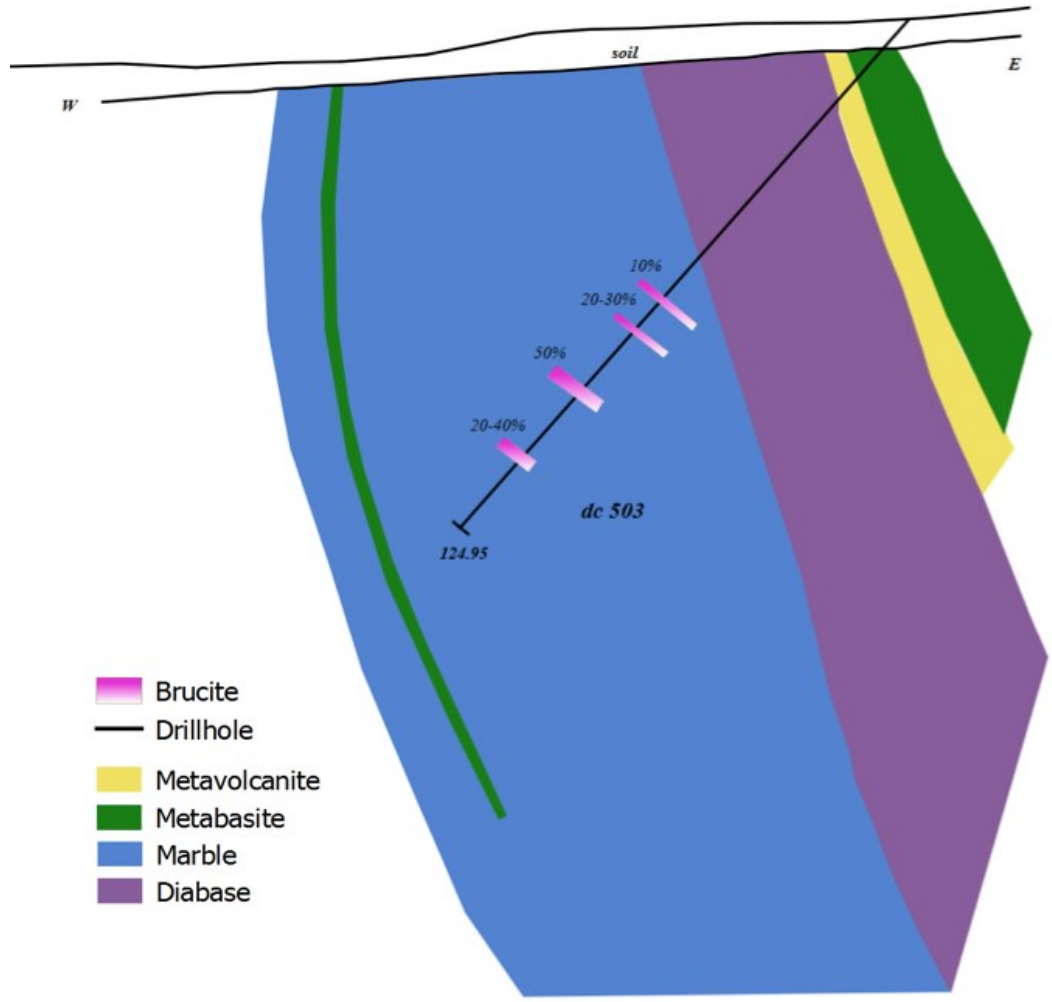

Figure 21. Lithological interpretation of the drill core 503. Mapped brucite (pink) is formed between the dolerite dyke and the older amphibolite. Percentages show the estimated brucite content during drill core mapping. Modified after SMA Mineral AB.

Brucite is heterogeneously scattered in drill core 504. The bedrock is exposed to near-vertical and complex metavolcanic and skarn intercalations (Fig. 22). Brucite is interpreted to originate from amphibolite and skarn. The deposit is heavily chloritized in the upper parts and has therefore been subjected to retrograde skarn alteration. Brucite in drill core 504 may petrogenetically be correlated with brucite in field site 2 (sample FS25).

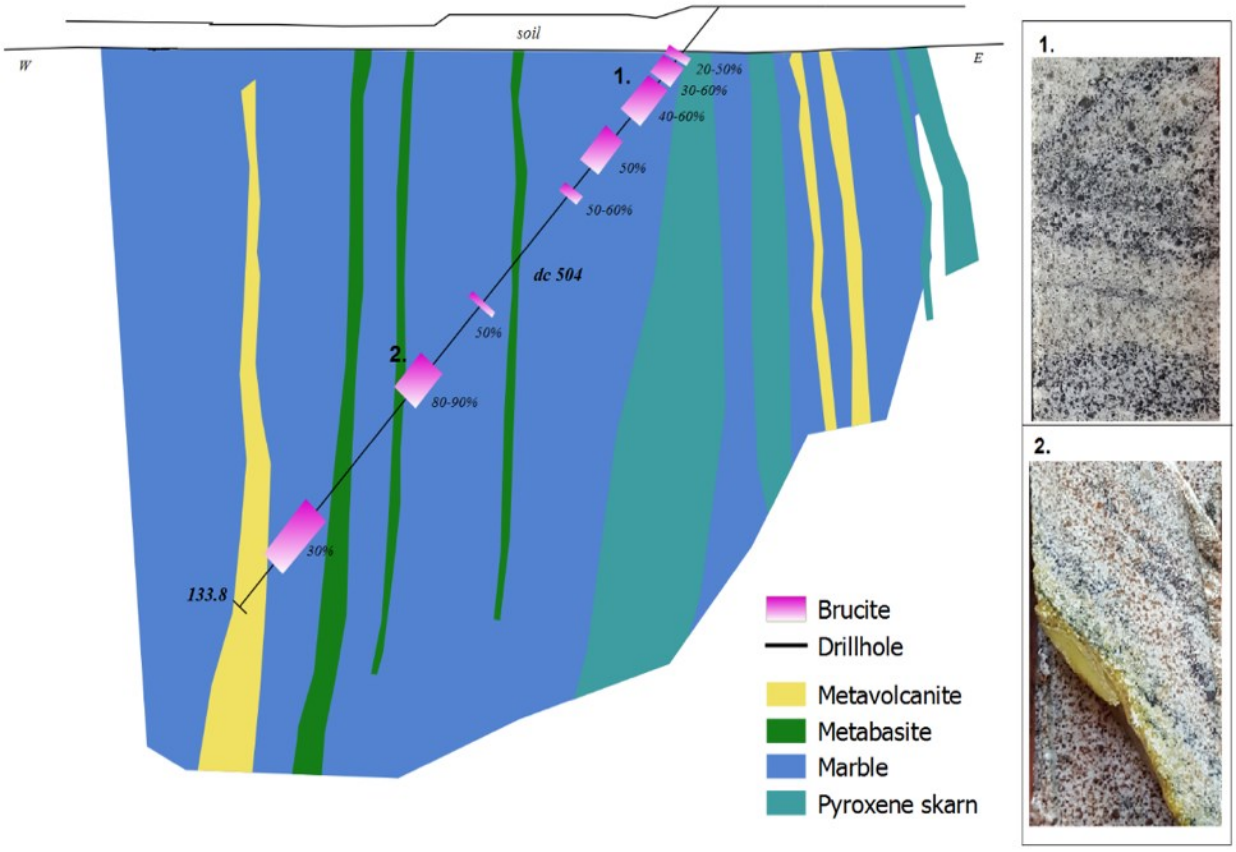

Figure 22. Lithological interpretation of the drill core 504 with core mapped brucite zones. Chloritized brucite marble at 17.2-25.75 m (No. 22-1) and brucite with antigorite at 78.1-86.8 m (No. 22-2). Percentages show the estimated brucite content during drill core mapping. Modified after SMA Mineral AB.

Brucite in drill core 507 is coherently distributed along skarn but absent close to quartzite (Fig. 23). Bands of magnetite appear occasionally with brucite. Brucite mineralization in drill core 507 is associated with the same amphibolite- and skarn-related brucite zone as in drill core 504 and field site 2.

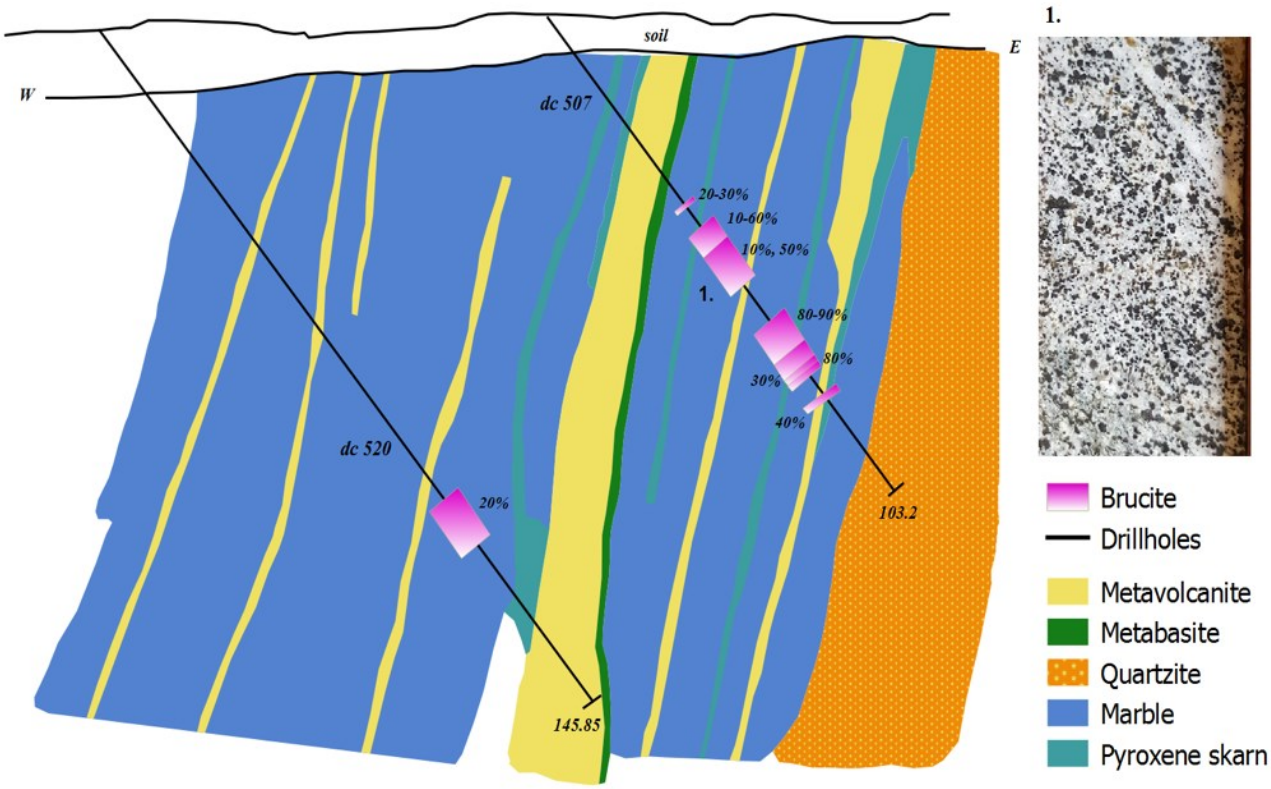

Figure 23. Lithological interpretation of the drill core 507 (and 520), where occurring brucite zones are found close to complex metavolcanites and skarn mineralizations. Percentages show the estimated brucite content during drill core mapping. Modified after SMA Mineral AB.

Drill core 515 is drilled through partially chloritized calcite marble, into a synvolcanic Horrsjö granite intrusion (Fig. 24). Brucite is formed by contact metamorphism between the dolomitic marble and the heated source. A shear zone (talc-chlorite schist) with some pyroxene skarn cuts the contact.

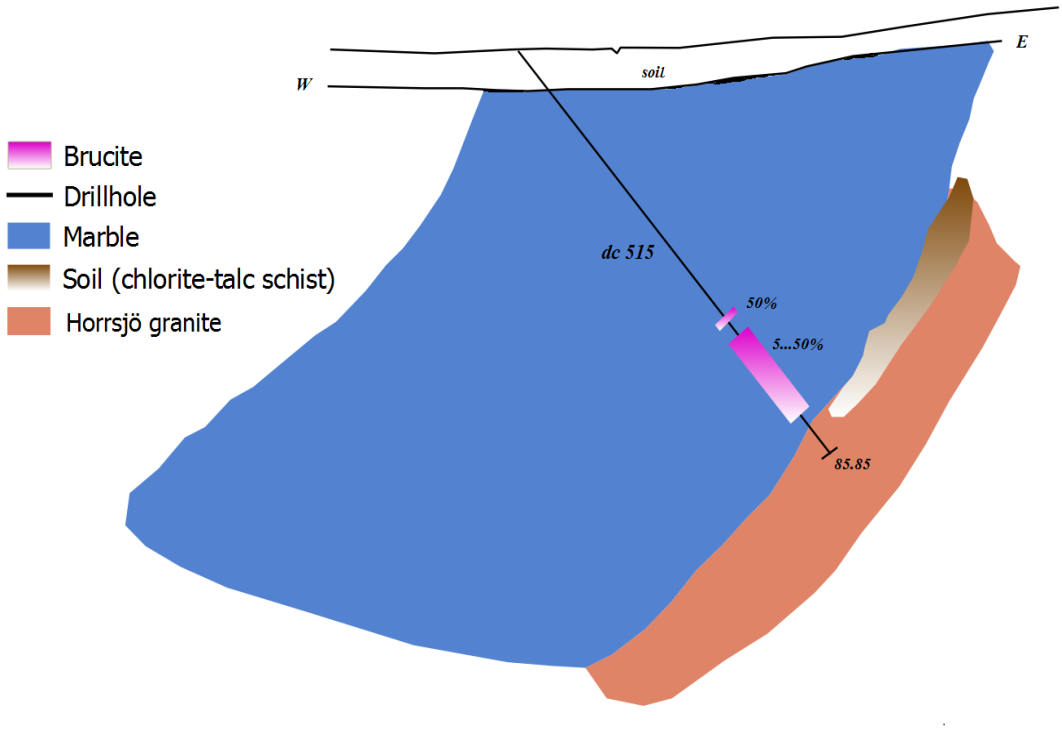

Figure 24. Lithological interpretation of the drill core 515 with encountered brucite. Brucite increases gradually towards the fractured contact. Percentages show the estimated brucite content during drill core mapping. Modified after SMA Mineral AB.

Drill core 518 is intersected by skarn and some felsic metavolcanites (Fig. 25). The drill core extends into a shear zone of weathered chlorite-talc schist and Horrsjö granite.

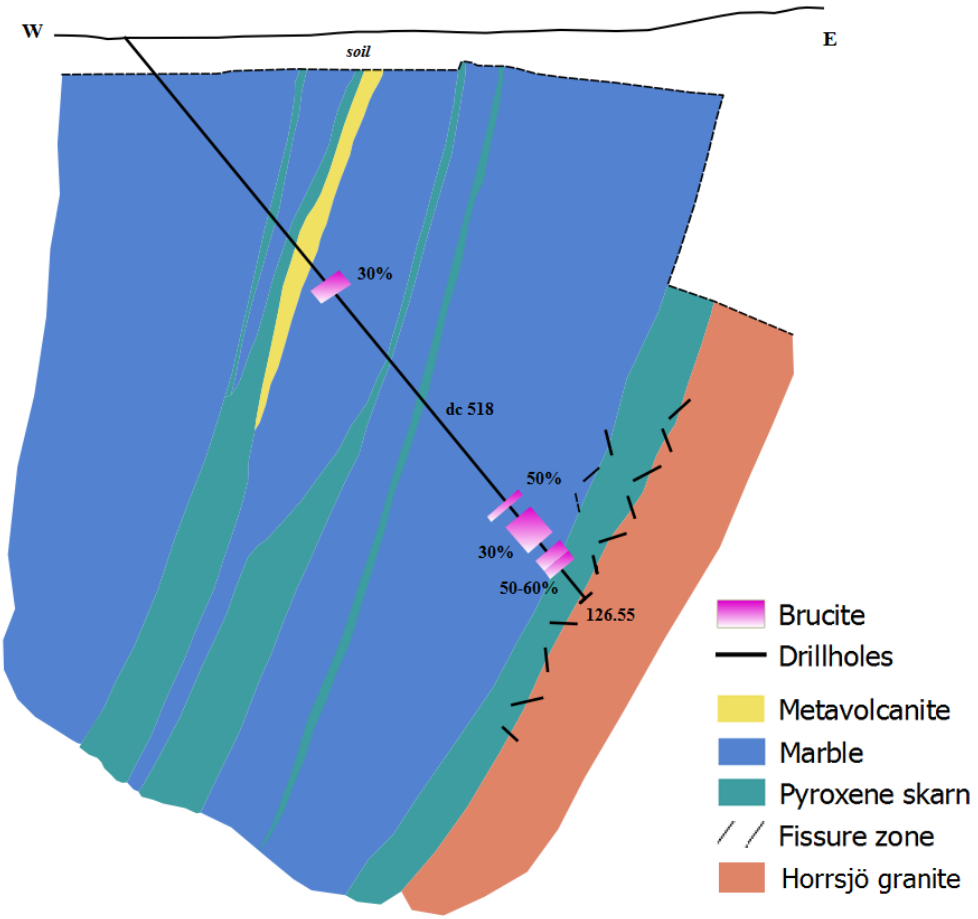

Figure 25. Lithological interpretation of the drill core 518. Brucite increases gradually towards skarn and a shear zone contact, located between marble and granite. Modified after SMA Mineral AB.

6.3.2 Brucite appearance in drill core series 600

Brucite in the examined drill cores of series 600 occurs mainly in the northwestern deposit. Brucite is encountered with some yellow antigorite, magnetite and chlorite in drill core 605 (Fig. 26). Drill core 606 is interpreted to be a continuum of the same mineralization zone, which is assumedly formed as a reaction product of the amphibolite dyke that intersects in the west. In drill cores 627 and 628, brucite appears

as sporadic and dark grains with some antigorite (Fig. 26). The genesis of brucite was not analyzed in microscale.

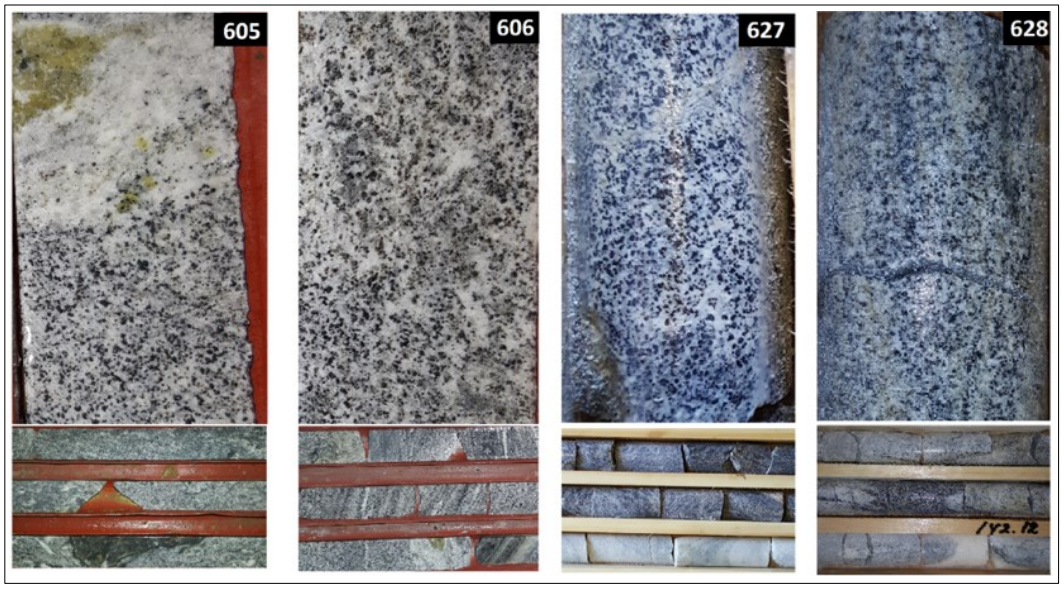

Figure 26. (605) Large antigorite grains (yellow) appear with small to medium grained black brucite. **(606)** Oriented dark brucite grains in white marble. **(627, 628)** Black brucite grains with some serpentine.

6.4 Petrographic analysis

Brucite is present in almost all analyzed thin sections. The mineral assemblages and the interpreted origin of brucite are visible in *Table 4-1* and *4-2*.

In plane polarized light brucite appears as light or dark brown grains with occasional pleochroism. Most brucite grains are spherical and euhedral, approximately 0.5-1 mm wide grains. Some morphological varieties of brucite show scaly-concentric texture (also referred to as “onion skin” texture). This texture appears in brucite when radially directed compressive stress has led to oriented brucite crystals kinking (Turner & Weiss, 1965). Brucite appears together with e.g. magnetite, diopside, chlinochlore/chlorite, hercynitic (Fe-rich) spinel, forsterite and/or serpentine in altered, dolomitic marble. Magnetite is often found in the core or rim of brucite, and

also as occasional small inclusions in dark brown brucite grains. The serpentine polymorph antigorite (Deer et al., 1997) is mainly present with brucite.

Table 4-1. Thin section analysis results with defined mineral assemblages and interpreted petrogenetic origin. Abbreviations: *brc = brucite (os = partly/only onion skin texture), chl = chlorite, di = diopside, for = forsterite, opq = opaques, phl = phlogopite, serp = serpentine, sp = spinel.* Brucite concentration (%) is estimated.

Sample	*Sampled at*	*Main minerals*	*Accessory minerals*	*Interpreted origin*	*Figure*
FS15	**S, field site 1**	**brc (60%, os)**	**for, sp, phl, opq, serp**	**serpentinization, dedolomitization**	**27**
FS25	**SE, field site 2**	**brc (60%, os)**	**opq, sp, serp, chl?**	**retrograde skarn, dedolomitization**	**28**
FS44	**NW, field site 4**	**brc (70%), opq**	**sp, mica/chl, di, feldspar**	**serpentinization**	**29**
FS92a	**W, field site 9**	**-**	**brc (20%), opq, chl**	**retrograde skarn**	**30a, b**
FS92c	**W, field site 9**	**brc (30%)**	**opq, chl/phl**	**retrograde skarn, chlorite breakdown**	
DC500.11	**Drill core 500, at 163.5 m**	**plagioclase**	**ilmenite, for, chl**	**skarn breccia**	
DC503.13	**Drill core 503, at 89.4 m**	**brc (30%), opq**	**chl, serp**	**serpentinization**	**31**
DC507.7	**Drill core 507, at 67.1-67.2 m**	**brc (50%, os), opq, serp**	**sp**	**serpentinization**	**32**
DC515.6	**Drill core 515, at 57.6-57.8 m**	**brc (30%, os), serp**	**for, chl, opq**	**hybrid (?)**	**33a**
DC518.13	**Drill core 518**	**opq, serp**	**chl**	**serpentinization**	**34**
DC534.4	**Drill core 534**	**-**	**chl, di, for**	**calc-silica reaction**	
DC535.6	**Drill core 535, at 46.0–46.1 m**	**brc (40%, os), opq**	**serp veins, chl (?)**	**serpentinization**	**35**
DC544.34	**Drill core 544, at 273.1-273.2 m**	**brc (50%)**	**opq, serp, sp, chl**	**serpentinization**	
DC606.2	**Drill core 606, at 11.4-11.5 m**	**brc (60%, os)**	**opq, feldspar**	**dedolomitization**	**36**
DC630.25	**Drill core 630, at 191.8-191.9 m**	**brc (50%)**	**opq, sp, serp, chl**	**hybrid (?)**	**37**

Table 4-2. Complementary thin sections provided by SMA Mineral AB.

Sample	*Sampled at*	*Main minerals*	*Accessory minerals*	*Interpreted origin*	*Figure*
515	**Drill core 515, at 65.0**	**brc (30%)**	**for/ serp, sp, opq**	**hybrid**	**33b**
515	**57.0**	**brc (60%)**	**opq**	**-**	
515	**74**	**-**	**brc (<20%)**	**-**	
528.13a	**31.6–34.9**	**chlorite**		**calc-silica reaction**	

6.4.1 Petrography of mapped field sites

Micro-scale interpretation of field site 1 (FS15)

Euhedral and partly subhedral brucite grains appear with pseudomorph forsterite and serpentine (Fig. 27a). Minor phlogopite is present with scaly-concentric pseudomorph brucite (Fig. 27b). SEM-EDS imaging shows further how spinel is abundant as small inclusions in magnetite (Fig. 27c). Some aluminum has supposedly been incorporated in serpentine from spinel, explaining the small peak of aluminum. Incorporated fluorine and calcium indicate the influence of hydrothermal fluids, giving forsterite a composition that resembles tremolite (see Appendix C).

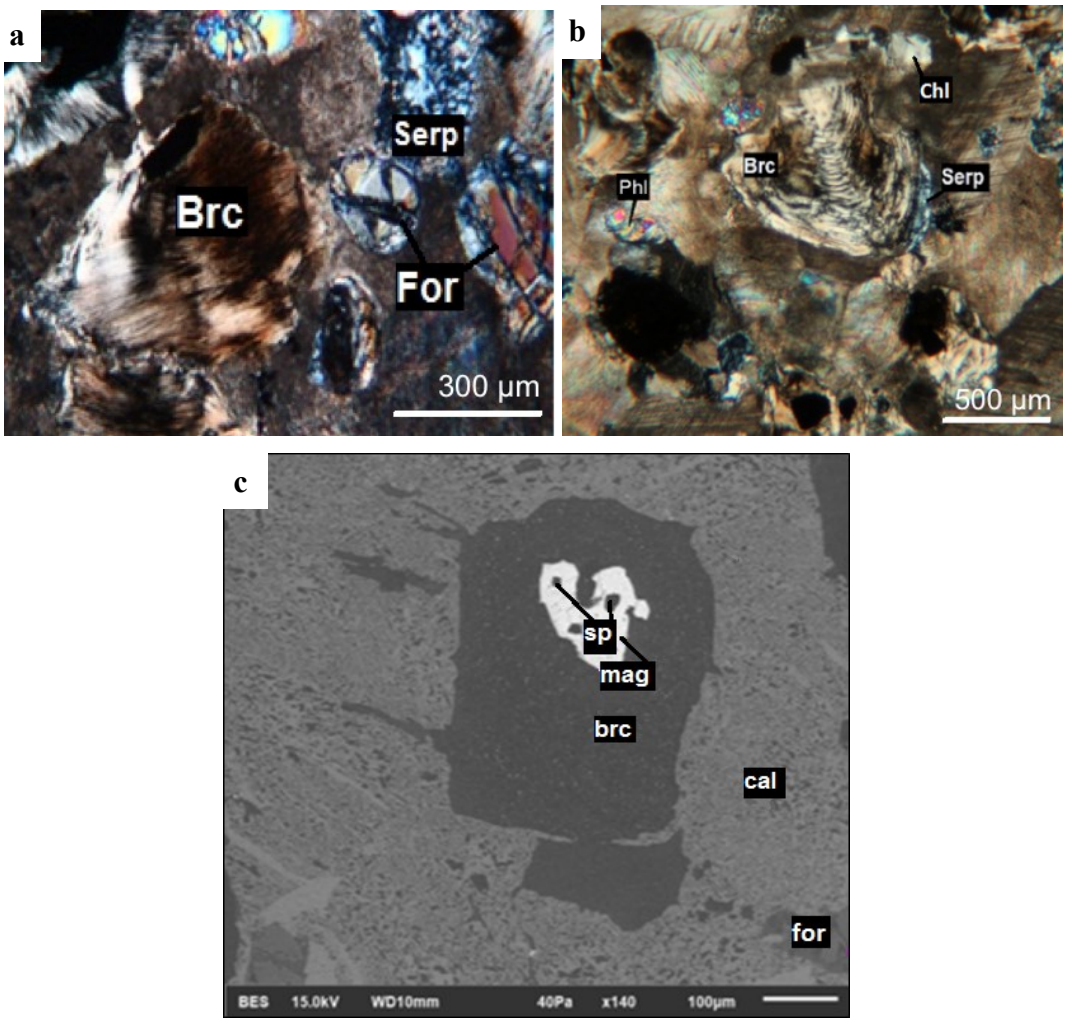

Figure 27. Sample FS15 (a) Brown, euhedral brucite (brc) grains with serpentinized forsterite (for) and serpentine (serp), XPL. **(b)** Scaly-concentric and spherical brucite pseudomorphs with minor phlogopite (phl) and serpentine. Chlorite (chl) appears in minor amounts, XPL. **(c)** SEM-EDS image of iron-rich brucite with a Mg-rich magnetite (mag) core and hercynitic spinel (sp) in a calcite (cal) matrix.

Micro-scale interpretation of field site 2 (FS25)

Brucite has a scaly-concentric texture with some opaque cores of magnetite. Remnant dolomite appears together with brucite (Fig. 28a, b). Brucite and magnetite appear in the contact of a secondary fluid rich calcite vein (Fig. 28c).

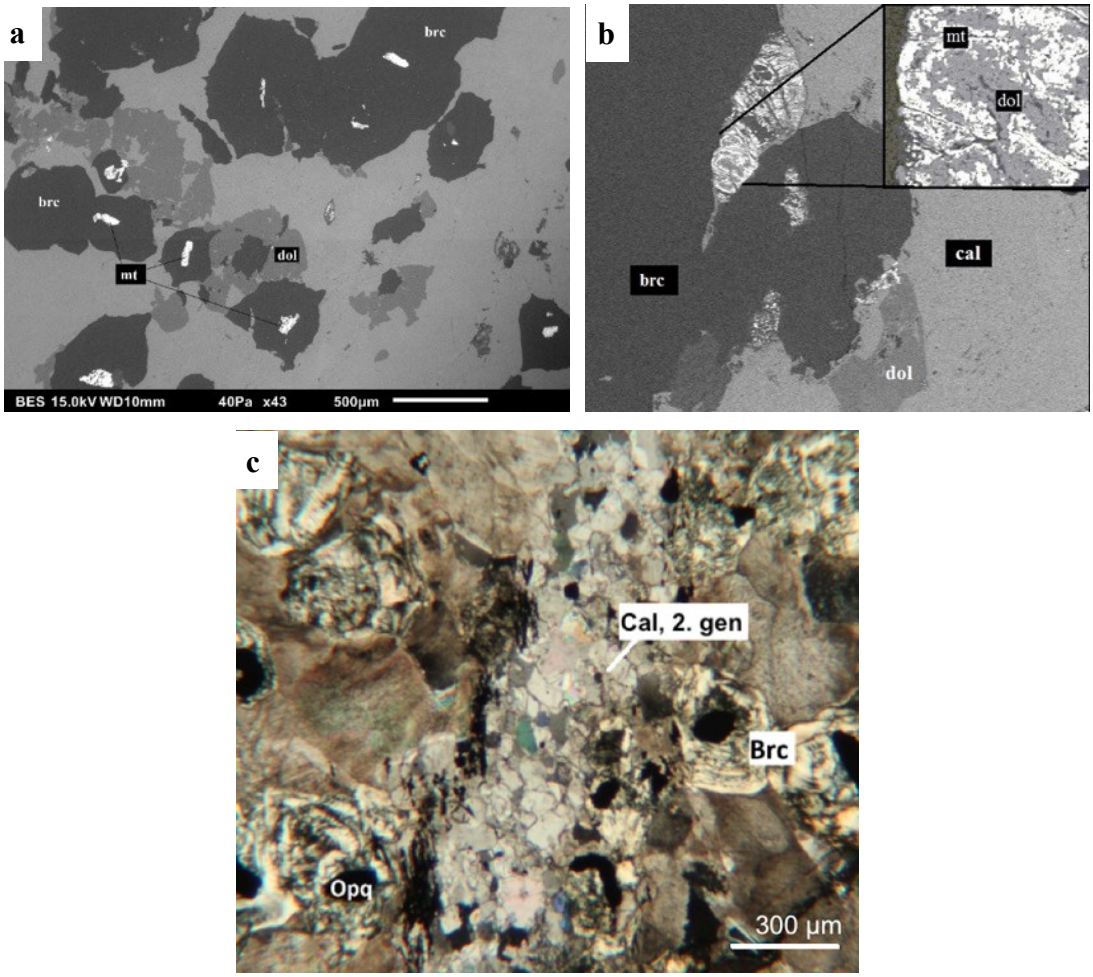

Figure 28. Sample FS25 (a), (b) SEM-EDS image of Fe-rich, remnant dolomite (dol), Mg-rich magnetite (mt) and brucite in calcite (cal). **(c)** Two generations of calcite marble with pseudomorph brucite and opaques (opq), XPL.

Micro-scale interpretation of field site 4 (FS44)

Brucite appears very dark due to substituted iron in the crystal lattice. Serpentine and spinel-overgrowth appear in minor quantities (Fig. 29a, b), whereas accessory opaque magnetite grains are abundant both in the rim and core of brucite. Brucite hosts a small serpentine grain in figure 29c, together with diopside and spinel.

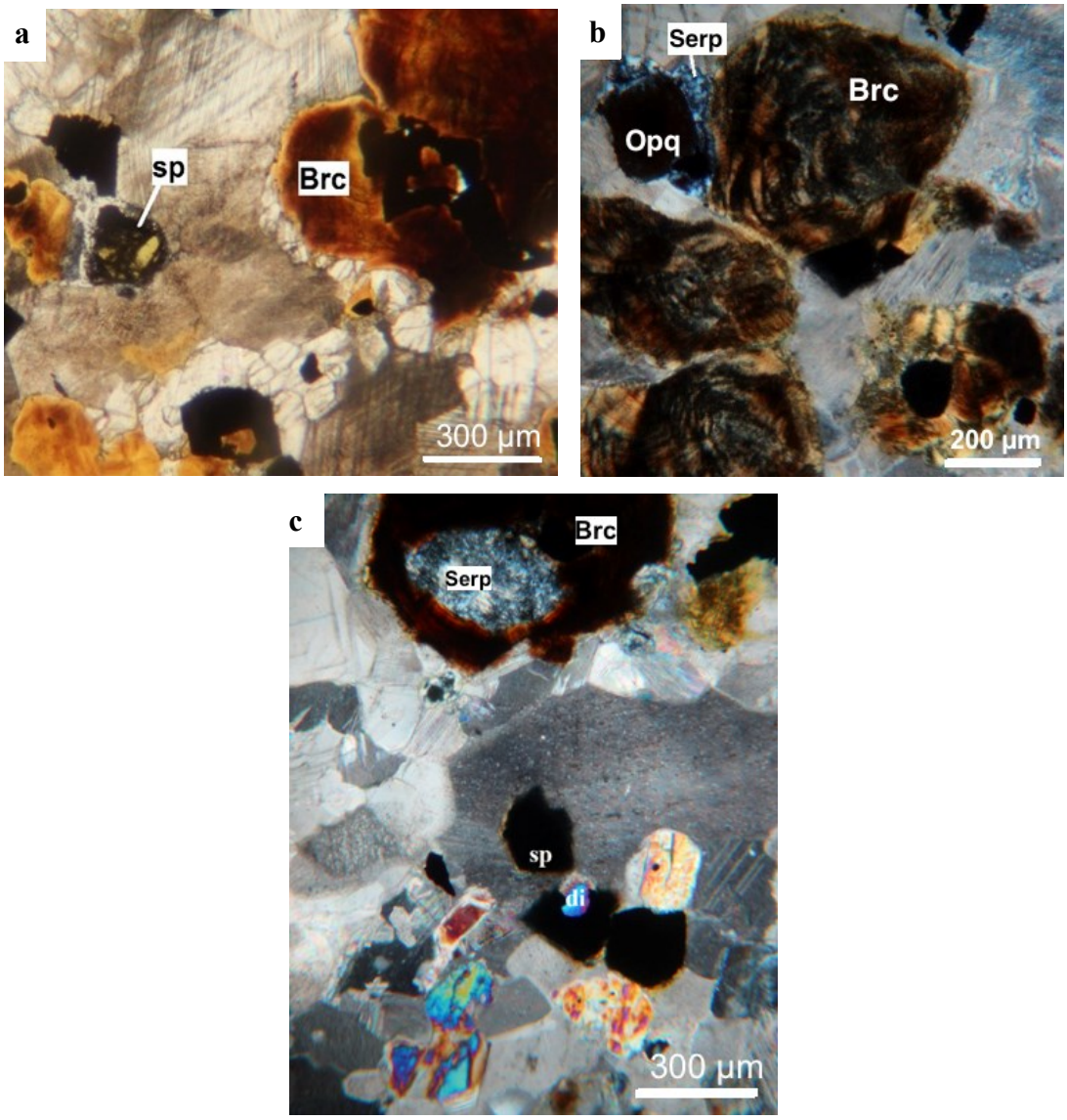

Figure 29. FS44 (a) Brucite (brc) and opaques with spinel-overgrowth (sp), PPL. **(b)** Minor serpentine (serp) with rounded iron-rich brucite grains and opaques, XPL. **(c)** Spinel (sp) and diopside (di) (or other calc-silica minerals) with brucite and serpentine, XPL.

Micro-scale interpretation of field site 9 (FS92a/FS92c)

Brucite has mineralized close to garnet-, epidote- and skarn with some sulphides and iron oxides. The marble is highly altered in retrograde conditions. Here brucite has formed during amphibolite alteration, since phlogopite and serpentine are present in minor quantities (Fig. 30). Brucite is very dark brown due to the high Fe-concentration

and coeval magnetite is common. This zone is interpreted to continue in drill cores 605 and 606.

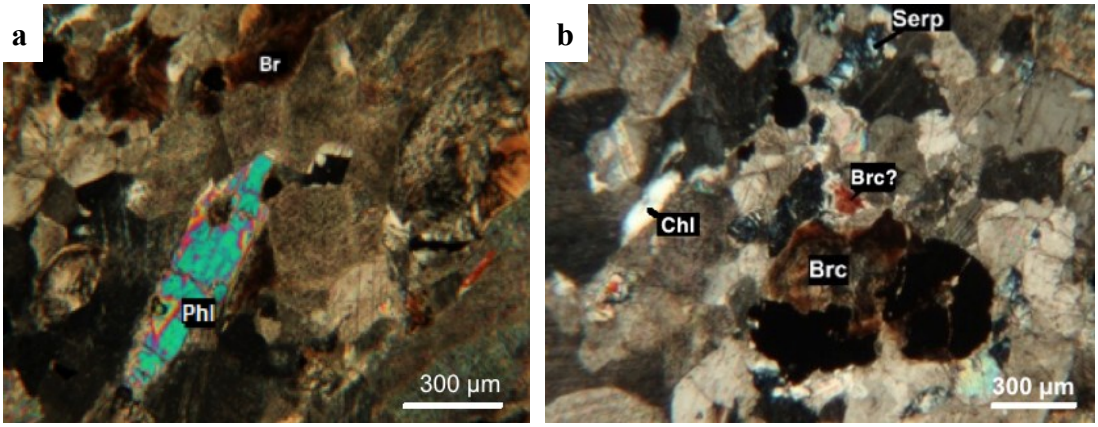

Figure 30. FS92a. (a) Fe-rich brucite, elongated phlogopite (phl) and accessory magnetite in altered marble, XPL. **(b)** Minor serpentine and chlorite (chl) with brucite, XPL.

6.3.1 Petrography of drill core series 500

Micro-scale interpretation of DC503.13

Magnetite appears as separate grains and as small inclusions in brucite in sample DC503.13 (Fig. 31a). Brucite is more anhedral than in the other samples and appears in two morphologically differing forms (Fig. 31b). Some brucite grains have onion-skin texture and an unknown core (titanite/sulphide?) with magnetite inclusions (Fig. 31c). Pseudomorph forsterite appears, in addition, with iron-rich brucite (Fig. 31d).

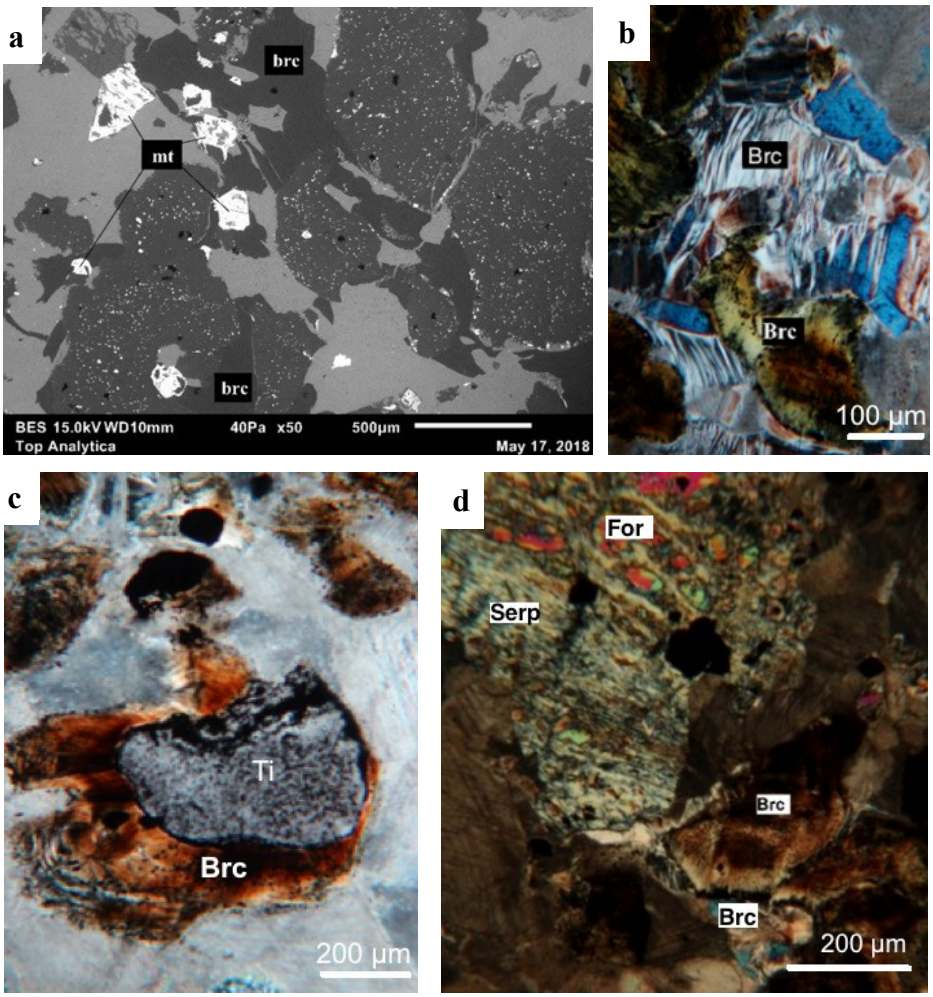

Figure 31. DC503.13. (a) SEM-EDS image of Mn-rich magnetite grains (mt) and small inclusions together with brucite in calcite marble. **(b)** Two morphological varieties of brucite, XPL. **(c)** Titanite (Ti) or a sulphide grain with magnetite inclusions in scaly-concentric brucite, XPL. **(d)** Serpentinized forsterite (for) with iron-rich brucite, XPL.

Micro-scale interpretation of DC507.7

Brucite appears with serpentine and some spinel-overgrowth (Fig. 32; sample DC507.7). Brucite is less iron-rich but magnetite grains are abundant. Some chlorite breakdown may have formed spinel and magnetite.

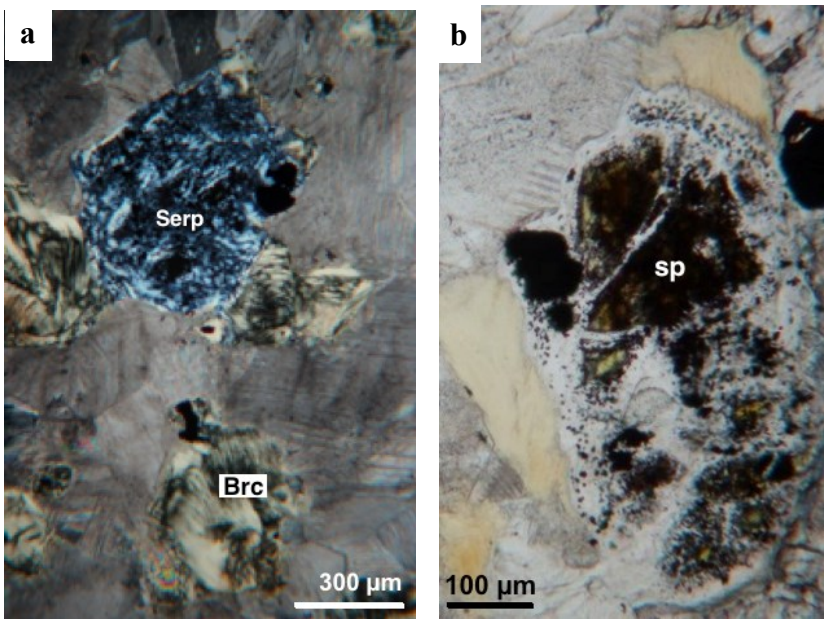

Figure 32. Sample DC507.7. **(a)** Subhedral brucite grains with serpentine (serp), XPL. **(b)** Spinel-overgrowth (sp) on magnetite, PPL.

Micro-scale interpretation of DC515.6 & DC515.65

Brucite appears with pseudomorph forsterite and antigorite in thin section DC515.6 (Fig. 33a). Mg-rich magnetite and remnant dolomite are present with brucite and forsterite in DC515.65 (Fig. 33b).

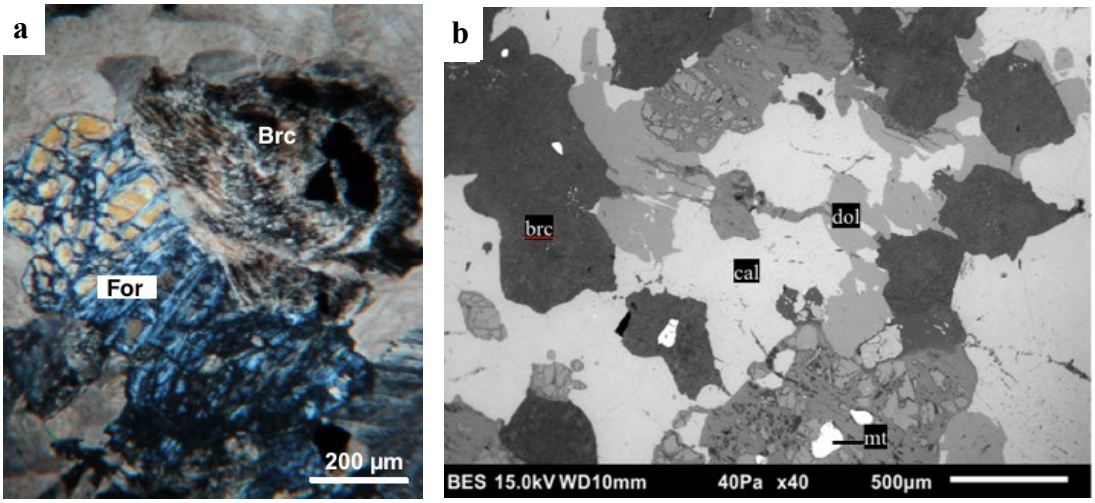

Figure 33. (a) Thin section DC515.6. Brucite together with forsterite pseudomorphs (for), XPL. **(b)** SEM-EDS image of DC515.65. Brucite, Mg-rich magnetite (mt) with some substituted titanium and remnant dolomite (dol) in a calcite matrix.

Micro-scale interpretation of DC518.13

Chlorite and Mg-rich magnetite appear together with strongly serpentinized marble (Fig. 34a; sample DC518.13). Some magnetite is abundant in the serpentine-rich marble matrix (Fig. 34b).

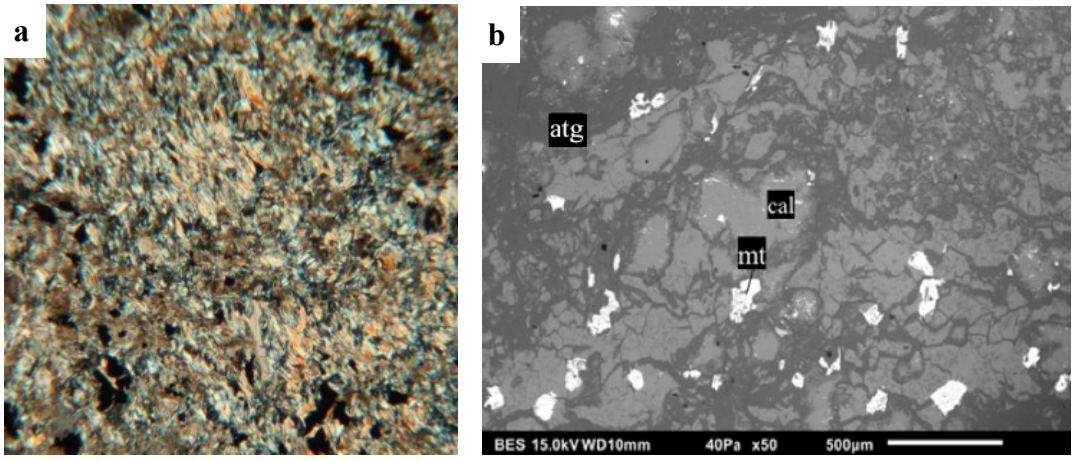

Figure 34. DC518.13. (a) Serpentinized marble (no scale) which indicates high inflow of fluids. **(b)** Magnetite (mt) and antigorite (atg) in a slightly dolomitic calcite (cal) marble.

Micro-scale interpretation of DC535.6

Brucite appears as subhedral periclase pseudomorphs with some opaque magnetite grains (Fig. 35a). Serpentine and brucite are abundant with secondary calcite veins (Fig. 35b).

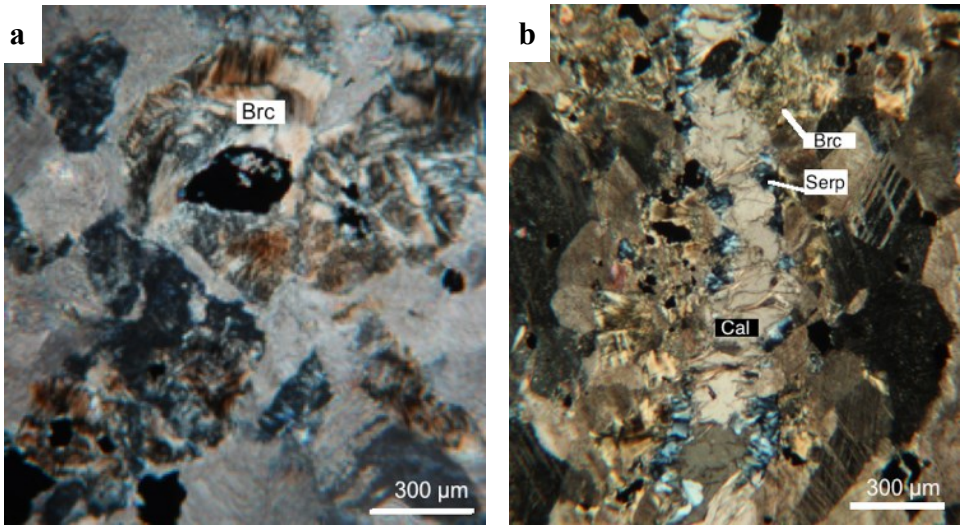

Figure 35. DC 535.6. (a) Pseudomorph brucite grains with opaques, XPL. **(b)** A secondary calcite vein with serpentine and brucite, XPL.

6.4.3 Petrography of drill core series 600

Micro-scale interpretation of DC606.2

Serpentine, brucite and feldspar (and other calc-silica minerals) are present in DC606.2 (Fig. 36a). Magnetite cores appear as opaques in pseudomorph brucite (Fig. 36b).

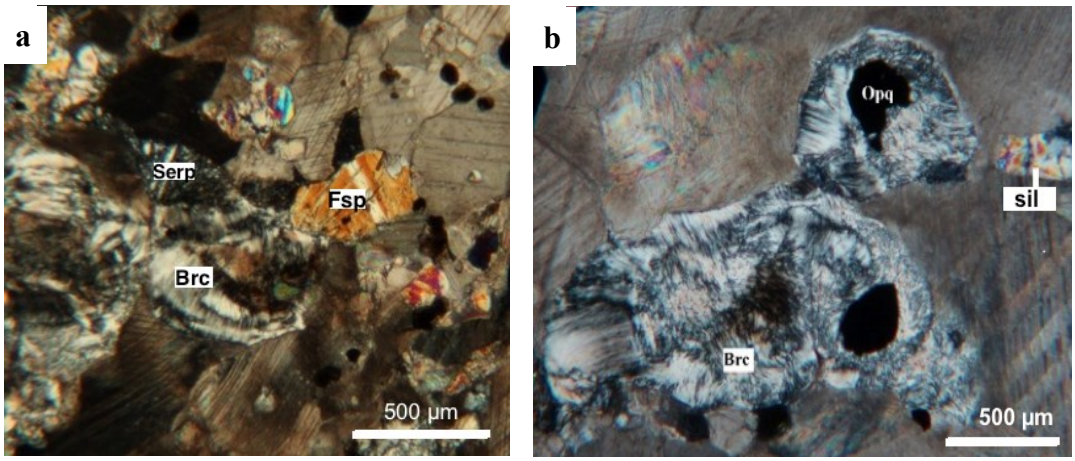

Figure 36. DC606.2 (a) Brucite with serpentine ingrowths and calc-silica minerals (fsp = feldspar). **(b)** Scaly-concentric brucite with opaque magnetite cores (sil = silica mineral).

Micro-scale interpretation of DC630.25

Brucite has a scaly-concentric texture and is formed from periclase in thin section DC630.25. Serpentine is present in minor quantities (Fig. 37a). Some brucite grains are partly brown, which would indicate partial iron substitution (Fig. 37b).

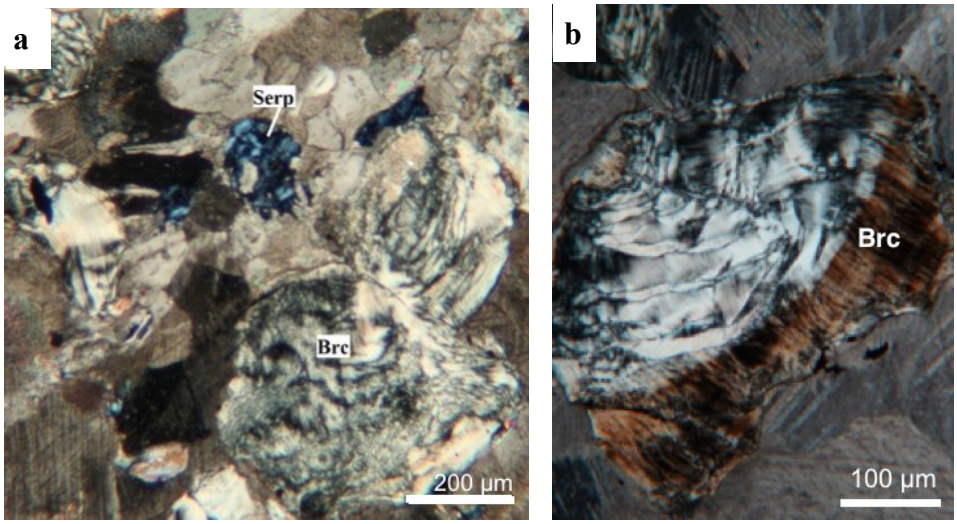

Figure 37. DC630.25. (a) Minor serpentine in pseudomorph brucite. **(b)** Brucite is partly brown and scaly-concentric.

7 DISCUSSION

The Gåsgruvan quarry has been subjected to regional metamorphism and contact metamorphism between plutonic intrusive rocks of pre-peak metamorphism and the crystalline marble. Later hydration of the deposit has given rise to brucite mineralization during the last metamorphic stage.

Brucite appears in both thick and thin curving mineralization zones in the Gåsgruvan open mine pit with a general strike of NW-SE. Most brucite zones are irregular and appear as intercalations in the marble without a foreseeable pattern. The largest concentrated brucite zones are abundant at the outer margins of the active mining area. Brucite appears with contaminated marble and felsic metavolcanics in the southern parts. In the west, a small brucite-rich zone is associated with pyroxene- and garnet-skarn and some oxides and sulphides. In northwest, brucite is present in an amphibolite

contact. A large brucite mineralization zone follows the southeastern margin and ends at a SiO_2-rich quartzite mineralization in the east.

7.1 Petrogenetic environment

7.1.1 Brucite morphology

Brucite appears in many morphologically varying shapes in this study. Brucite with a scaly-concentric (onion-skin) texture is defined as retrograde pseudomorphs of periclase. Some brucite appears, in return, as grains with later kinking textures and is not associated with a pseudomorphous origin (Turner & Weiss, 1965). It is difficult to determine if dark brown brucite grains originate from periclase, since the scaly-concentric texture is less distinguishable in these grains. The spherical shape cannot be used as an indicator for periclase hydration. This is due to the fact that brucite generally appears as spherical grains in calcitic marble and forms angular grain boundaries in dolomitic marble which conforms to the marble cleavage (Øvereng, 2000 and references therein).

Mn-rich brucite grains have been identified with visible periclase cores in Gåsgruvan (Magnusson, 1925). However, no periclase was found in any of the analyzed thin sections, which indicates that external H_20-rich fluids have been mobile enough to complete the retrograde hydration reaction (reaction II in Chapter 4.2.1).

7.1.2 The role of forsterite, serpentine and magnetite during serpentinization

Brucite is often abundant with pseudomorph forsterite, opaque grain cores and phyllosilicates such as chlorite, mica and/or the serpentine polymorph antigorite. Brucite and antigorite are presented as reaction products of forsterite alteration in this study, but forsterite is often absent in samples where antigorite is present (e.g. samples FS44; FS92a; FS92c; DC507.7).

Some serpentines in northern Sweden have been reportedly formed from tremolite and diopside, which may also apply to serpentines in Gåsgruvan. In addition, serpentine can form by hydrothermal solutions directly from dolomite, without the intermediate stage of forsterite (Frietsch, 1984 and references therein). This suggests that serpentine may be a result of dolomite alteration and not forsterite serpentinization in this study. In contrast, brucite may have progressively replaced the whole forsterite grain and retained its original crystal shape (Øvereng, 2000 and references therein). Brucite may therefore act as a better indicator of serpentinization than serpentine.

The opaque cores and inclusions in brucite are defined as magnetite. Magnetite is further defined as a late reaction product of serpentinization. Interestingly, magnetite is also abundant in most dolomite-derived brucite pseudomorphs in this study. This indicates that magnetite may have been abundant early in the bedrock by deposition as a primary chemical precipitate, such as in northern Sweden (Frietsch, 1984). Thus, magnetite may not only be a reaction product of serpentinization in Gåsgruvan.

7.2 Skarn mineralization

Gåsgruvan skarns correspond with the SVALS endmember type of skarns, such as the base metal sulphide deposits of e.g. Garpenberg (see Appendix A). SVALS skarns are strata-bound, volcanic-associated, limestone-skarn sulphide deposits. These skarns host marble beds as inliers in metavolcanics, with abundant Mg-rich tremolite-diopside skarn and dolomitic zones (Allen et al., 1996). Footwall Mg-alteration of this type of skarn resemble the intense brucite mineralization zone at the eastern part of Gåsgruvan.

Brucite, periclase, serpentine and phlogopite represent some typical Mg-skarns and are usually absent in most other types of skarn. Since both periclase and serpentine fall under the general term of Mg-skarns, brucite of Gåsgruvan may be a hybrid of both serpentinization and dedolomitization.

7.3 Comparison between brucite-rich zones

Brucite has been influenced by both forsterite and periclase alteration in the southern and southwestern Gåsgruvan (field site 1; sample FS15). In southeast, a large brucite zone is located between drill cores 504 and 507, and field site 2. The upper part of this zone is strongly chloritized which may indicate retrograde pyroxene skarn alteration. Brucite appears as iron-depleted, light spherical pseudomorphs with remnant dolomite. Wennerström (2015) suggested that the remnant dolomite is associated with Mg-rich fluids from younger granitic magmas, which dolomized the marble. However, it appears that the bedrock has originally been dolomitic due to subaqueous Mg-alteration. The later dedolomitization during contact metamorphism has formed calcite and left some remnant dolomite. In addition, some iron-rich, forsterite altered brucite (DC503.13) occurs close to pre-peak metamorphic amphibolite and a younger dolerite dyke in the eastern deposit.

In the west (samples FS92a; FS92c; DC606.2), brucite is associated with periclase alteration and some calc-silica reactions, whereas no serpentinization has taken place here. Brucite in the northwestern quarry is very brown and magnetite-rich and formed in the contact of iron-rich amphibolite (sample FS44) together with spinel. Spinel is formed as a spinel-hercynite overgrowth on low-grade magnetite during serpentinization. Spinel may also be a result of chlorite breakdown, where iron partitions into spinel and magnetite (Bucher & Grapes, 2011). Minor diopside occurs here which may have partly altered to serpentine.

7.4 The role of shear zones

Shear zones on the western and eastern margin of Gåsgruvan (Fig. 38), which contain e.g. chlorite, talc, limonite and magnetite (drill core data of SMA Mineral AB), may have carried H_2O-fluids into the deposit (Wennerström, 2015).

In the north-central parts of the deposit (drill core 515 and 518) brucite is formed near a fracture zone, separated by Horrsjö granite, pyroxene skarn and marble. The marble is strongly serpentinized, chloritized and oxidixed, indicating that external fluids have

been present here. CO_2 that forms during dedolomitization has suggestively left the system through the same shear or fracture zones, in the same way as in the Nantei mine in Korea (Watanabe, 1935).

Figure 38. Small shear zone between mafic brecciated amphibolite (left) and marble (right). The shear zone may have carried fluids into the marble deposit, forming hydrated Mg-rich minerals such as brucite. Image from field site 2.

7.5 Distribution of brucite

Brucite is mainly distributed in a crescent structure in south and southeast, which follows a curving pattern that continues from southeast towards northwest. The 3D-model gives good indications on both magnitude and orientation of the brucite distribution even if these zones are based on bold interpretations.

The crescent mineralization zone in the southeast appears to be the largest brucite mineralization zone in Gåsgruvan, where the bedrock is exposed to very complex mineralizations. Fluids may have entered this mineralization zone from the south, since brucite appears deep in some of the southbound drill cores.

Complex intercalations of metavolcanics and skarn, especially in the west and in the central deposit, may explain the scattered nature of brucite. This indicates that the hydrothermal fluids could not penetrate through all joints and fissures in the marble. The central and northern mineralization zones are most scattered since the interpretations are based on limited core data. No larger correlations are made here, since these interpretations would not assumedly correspond with reality.

Zones with MgO > 5.5% correlate well with the modelled brucite zones. The MgO-rich areas and the interpreted brucite zones extend from southeast to northwest (Fig. 39), parallel to the marble foliation. The anomalies differ mainly in northeast, where no zones were modelled due to unreliable data from disposed drill cores.

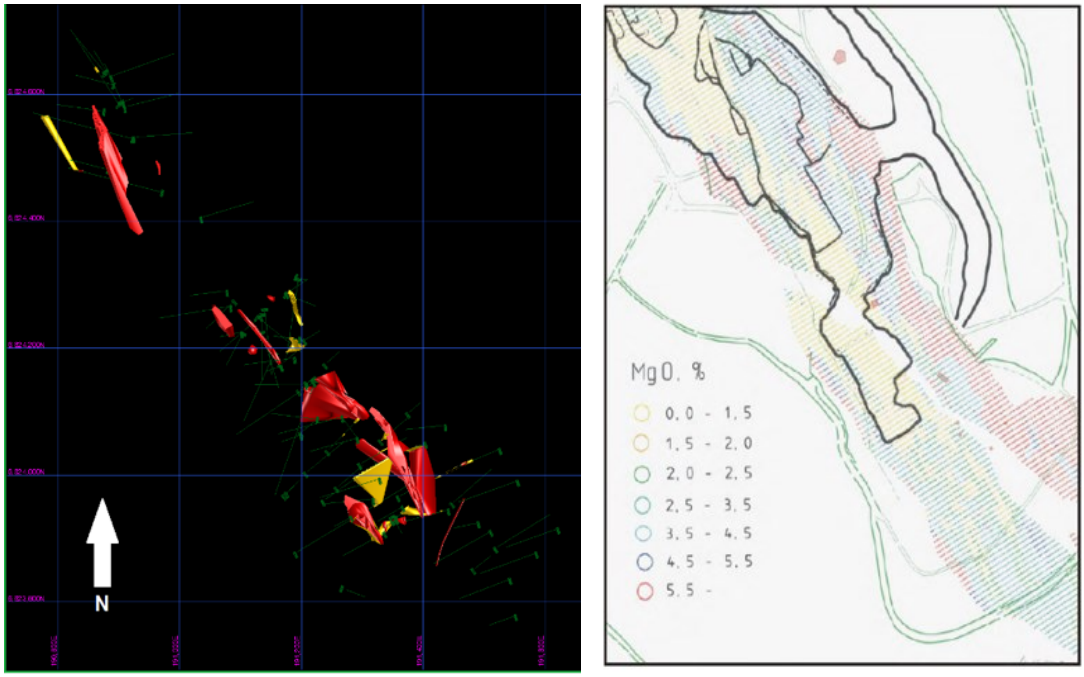

Figure 39. Modelled brucite zones correlate well with high concentrations of XRF-mapped MgO (MgO elemental map after Karlsen, 2000).

7.6 Metamorphic conditions

The metavolcanics in western Bergslagen contain blue quartz megacrysts, implying that the local rocks have reached greenschist facies metamorphism. Extensive zones

of amphibolite facies occur in the Filipstad area, since these megacrysts are not found in higher grade rocks (Oen, 1987 and references therein). Björk (1986) identified sillimanite and cordierite at the Yngen islands, assessing this peak metamorphic condition.

The abundance of both thick and thin lamellae (mechanical e-twinning) in Gåsgruvan marble indicates deformation conditions of at least T>400°C (Ferrill et al., 2004 and references therein). The presence of periclase makes it evident that Gåsgruvan has been subjected to temperatures of at least c. 600°C. Wennerström (2015) assumed that the regional greenschist facies has risen locally to amphibolite facies due to the influence of intrusive igneous rocks. The mineral assemblage of spinel + forsterite + diopside indicates peak metamorphic temperatures of 640-720°C (OMYA, 2014).

7.7 Constraints

Diamond drilling is usually carried out with the aim to prospect exploitable ores and industrial minerals. Brucite is an unwanted tailing product which means that many brucite-enriched zones have not been drilled. It is also difficult to interpret larger zones and the petrogenetic origin for brucite in drill cores where data is restricted, such as in drill core 630. During core and field mapping, brucite may be mixed with minerals such as magnetite, chlorite, humite or phlogopite due to the similar appearance. The estimation may not correlate with reality and therefore low elevations of brucite were generally disregarded in this thesis. In addition, limited satellite connection and ongoing mining constrained detailed field work.

3D-modelling was mainly constrained due to the utilized MgO/SiO_2 ratio which did not take into account silica-depleted and Mg-enriched minerals such as dolomite ($CaMg(CO_3)_2$). The ratio of MgO/SiO_2 was not used as a single parameter for any modelled brucite zones due to the high abundance of dolomite in the deposit.

Microscale analysis was limited since the total number of thin sections was small and each thin section represented a large area of the deposit. In addition, SEM-EDS

analysis was constrained since the hydroxide group of analyzed minerals was not detectable, aggravating identification of hydrous mineral assemblages.

8 CONCLUSIONS

Gåsgruvan is subjected to brucite mineralization, which is caused by hydration of the marble deposit during the last metamorphic stage. Scaly-concentric brucite is formed due to dedolomitization during periclase hydration and iron-rich, brown brucite is associated with forsterite alteration in close contact with mafic intrusions. Retrograde conditions have also given rise to other hydrous minerals such as chlorite and phlogopite. 3D-modelling of correlated brucite mapped zones shows that brucite forms a crescent form in the southern and southeastern part of the deposit. This zone continues deep into the marble lens towards south. Brucite follows a curving pattern which appears in the southeastern deposit and continues towards northwest. Brucite is generally present in near contact with large amphibolite intrusions that margin the deposit in west and east. Brucite appears very scattered in the central and northern parts of the quarry. Studies conducted with lithological drill core profiles show that brucite is associated with some synorogenic granitic intrusions and pyroxene skarn. Shear zones may have carried external fluids to the deposit.

9 FUTURE STUDIES

For future work, preparation of more thin sections and more micro-scale analysis is needed to understand detailed relations between brucite zones and rock intrusions, especially in series 600. Isotope and fluid inclusion studies may give better indication of timing and influence of fluid alteration. 3D-modelling results can be extended, and more correlations may be found by utilizing all core data, especially from disposed drill cores.

REFERENCES

Allen, R. L., Lundström, I., Ripa, M., Simeonov, A. & Christofferson, H. (1996). Facies analysis of a 1.9 Ga, continental margin, back-arc, felsic caldera province with diverse Zn-Pb-Ag-(Cu-Au) sulfide and Fe oxide deposits, Bergslagen region, Sweden. Economic Geology 191, 979–1008 pp.

Anthony J. W., Bideaux R. A., Bladh, K. W. & Nichols, M. C. (Eds.) (2001-2005). Handbook of Mineralogy; brucite. Mineralogical Society of America, Chantilly, VA 20151-1110, USA (WWW-document) (3.7.2018).

Ashley, P. M. (1975). Opaque mineral assemblage formed during serpentinization in the Coolac ultramafic belt, New South Wales. Journal of the Geological Society of Australia. 22(1). 91–102 pp.

Beunk, F. F. & Kuipers, G. (2012). The Bergslagen ore province, Sweden: Review and update of an accreted orocline, 1.9-1.8 Ga BP. Precambrian Research 216-219. 95–119 pp.

Björk, L. (1986). Beskrivning till berggrundskartan Filipstad NV. Sveriges Geologiska Undersökning. Serie Af Nr 147. 110 p.

Bucher, K. & Grapes, R. (2011). Petrogenesis of Metamorphic Rocks. (8th ed.) Springer-Verlag Berlin Heidelberg. 428 p.

Deer, W.A., Howie, R.A. & Zussman, J. (1997). Rock-Forming Minerals: Orthosilicates, Volume 1A. The Geological Society. 932 p.

Ferrill, D. A., Morris, A. P., Evans, M.A., Burkhard, M., Groshong Jr., R. H. & Onasch, C.M. (2004). Calcite twin morphology: a low-temperature deformation geothermometer. Journal of Structural Geology. Acta 26: 1521–1529 pp.

Frietsch, R. (1984). Formation of Mg-bearing magnetite and serpentine in skarn iron ores in northern Sweden. Geologiska Föreningen i Stockholm Förhandlingar, 106(3), 219–230 pp.

Gorbatschev, R. (2004). The Transscandinavian Igneous Belt – introduction and background. In: K. Högdahl, U.B. Andersson & O. Eklund (eds.): The Transscandinavian Igneous Belt (TIB) in Sweden: a review of its character and evolution. *Geological Survey of Finland Special Paper 37*. 9–15 pp.

Huang, R., Lin, C-T., Sun, W., Zhan, W. & Zhu, J. (2017). The production of iron oxide during peridotite serpentinization: Influence of pyroxene. Geoscience Frontiers. Vol. 8, Issue 6. 1311–1321 pp.

Högdahl, K., Andersson, U. B. & Eklund, O. (eds.) (2004). The Transscandinavian Igneous Belt in Sweden: A review of its character and evolution. Geological Survey of Finland Special Paper 37. 125 p.

Högdahl, K. & Jonsson, E., (2004). The Horrsjö complex in the Bergslagen ore province: a Palaeoproterozoic caldera with a mineralised rim? In J. Mansfeld (ed.): The 26th Nordic Geological Winter Meeting. Abstract Volume. GFF 126. 23 p.

Högdahl, K., Jonsson, E. & Selbekk, R.S. (2007). Geological relations and U–Pb geochronology of Hyttsjö granites in the Långban-Nordmark area, western Bergslagen, Sweden. GFF. Volume 129. 43–54 pp.

Jarl, L.-G. & Johansson, Å. (1988). U-Pb zircon ages of granitoids from the Småland-Värmland granite-porphyry belt, southern and central Sweden. Geologiska Föreningens i Stockholm Förhandlingar 110. 22–28 pp.

Jansson, N.F. & Allen, R.L. (2012). Timing and setting of skarn and iron oxide formation at the Smältarmossen calcic iron skarn deposit, Bergslagen, Sweden. Springer-Verlag. Miner Deposita 48. 313–339 pp.

Jeol (2018). https://www.jeol.co.jp/en/products/detail/JSM-IT100.html. (WWW-document) (06.12.2018).

Karlsen, T. A. (2000). Resources for GKAB at Gåsgruvan, Filipstad. 31 p.

Lahtinen, R., Korja, A. & Nironen, M. (2005). Paleoproterozoic tectonic evolution. In: Lehtinen, M., Nurmi, P.A., Rämö, O.T., (eds.). Precambrian Geology of Finland-Key to the Evolution of the Fennoscandian Shield. Elsevier, Amsterdam, Developments in Precambrian Geology, 14, 481–532 pp.

Lundegårdh, P. (1987). Beskrivning till bergartskartan Filipstad SV. Sveriges Geologiska Undersökning. Serie Af Nr 157. 77 p.

Magnusson, N. H. (1925). Persbergs malmtrakt och berggrunden i de centrala delarna av Filipstads bergslag. Kungliga kommerskollegium: Beskrivning av mineralfyndigheter 2. 231 p.

Meinert, D. L. (1992). Skarns and Skarn Deposits. Geoscience Canada. Vol. 19. Nr. 4. 145–158 pp.

Moody, J.B. (1976). Serpentinization: a review. Lithos 9. 125–138 pp.

Mottana, A., Crespi, R. & Liborio, G. (1983). The MacDonald Encyclopedia of rocks and minerals. MacDonald & Co (Publishers) Ltd. London & Sydney. 607 p.

Müller, T., Baumgartner, L. P., Foster, JR & Bowman, J.R. (2009). Crystal Size Distribution of Periclase in Contact Metamorphic Dolomite Marbles from the Southern Adamello Massif, Italy. Journal Of Petrology. Vol. 50, Nr. 3. 451–465 pp.

Oen, I. S. (1987). Rift-related igneous activity and metallogenesis in SW Bergslagen, Sweden. Precambrian Research 35. 367–382 pp.

OMYA (2011). Status on geology and mining, Gåsgruvan calcite quarry. In-house report.

OMYA (2014). Brief excursion into mineral microstructures from Persberg. In-house report.

Øvereng, O. (2000). Granåsen, a dolomite-brucite deposit with potential for industrial development. NGU Bulletin 436. 75–84 pp.

Pekkala, Y. (1985). Petrography, geochemistry and mineralogy of the Precambrian metasedimentary carbonate rocks in North Kuusamo, Finland. Geological Survey of Finland, Bulletin 332. 62 p.

Sandström, F, Lorin, T. & Strand, U (2009). Geologi och mineralogi i Gåsgruvefältet, Filipstad. Litofilen Årgång 26 Nr. 1. 23 p.

Schumann, W. (1992). Minerals of the world. Sterling Publishing Company, Inc. 232 p.

Shaikh, N.A., Karis, L., Snäll, S., Sunberg, A. & Wik, N. (1989). Kalksten och dolomit i Sverige: Del 2. Mellersta Sverige. 122–124 pp.

SMA Mineral AB (2018). https://smamineral.se/sv/facility/gasgruvan-3/ (WWW-document) (5.11.2018).

Stephens, M. B., Ripa, M., Lundström, I., Persson, L., Bergman, T., Ahl, M., Wahlgren, C-H., Persson P-O., & Wickström, L. (2009). Synthesis of the bedrock geology in the Bergslagen region, Fennoscandian shield, south-central Sweden. Sveriges Geologiska Undersökning. 259 pp.

Stuge, B. (1986). Gåsgruvans geologi 1986. In-house report.

Sveriges Geologiska Undersökning (Geological Survey of Sweden) (2018). http://apps.sgu.se/kartgenerator/maporder_sv.html (WWW-document) (29.10.2018).

Terry, R. D., & Chilingar, G. V. (1955). Summary of "Concerning some additional aids in studying sedimentary formations," by M. S. Shvetsov. Journal of Sedimentary Research, 25(3). 229–234 pp.

Turner, F. (1965). Note on the genesis of brucite in contact metamorphism of Dolomite. Beiträge zur Mineralogie und Petrographie 11. 393–397 pp.

Turner, F. & Weiss, L. E. (1965). Deformational kinks in brucite and gypsum. Proc. Nat. Acad. Sci. U.S. 54. 359–364 pp.

Watanabe, T. (1935). On the Brucite-Marble (Predazzite) from the Nantei Mine, Suian, Tyôsen (Korea): The Geology of the Suian Gold Mining District (1st Report). Hokkaido Imperial University. Ser.4, Geology and mineralogi, 3(1): 49–59 pp.

Wennerström, A. (2015). Brucite mineralization in a hydrothermally altered carbonate system, in the marble of Gåsgruvan Bergslagen area, central Sweden. Unpublished thesis for Master of Science degree in Geology. University of Gothenburg. 55 p.

Winter J. D. (2014). Principles of Igneous and Metamorphic Petrology. (2nd ed). Pearson Education Limited. 737 p.

Åberg, G., Bollmark, B., Björk, L., & Wiklander, U. (1983). Radiometric dating of the Horrsjö granite, south central Sweden. GFF, vol (105), 78–81 pp.

APPENDICES

Appendix A. Petrogenetic illustration of the Bergslagen volcanic complex and the two main skarn formation types (Allen et al., 1996). The Gåsgruvan skarns correspond to the SVALS type skarns.

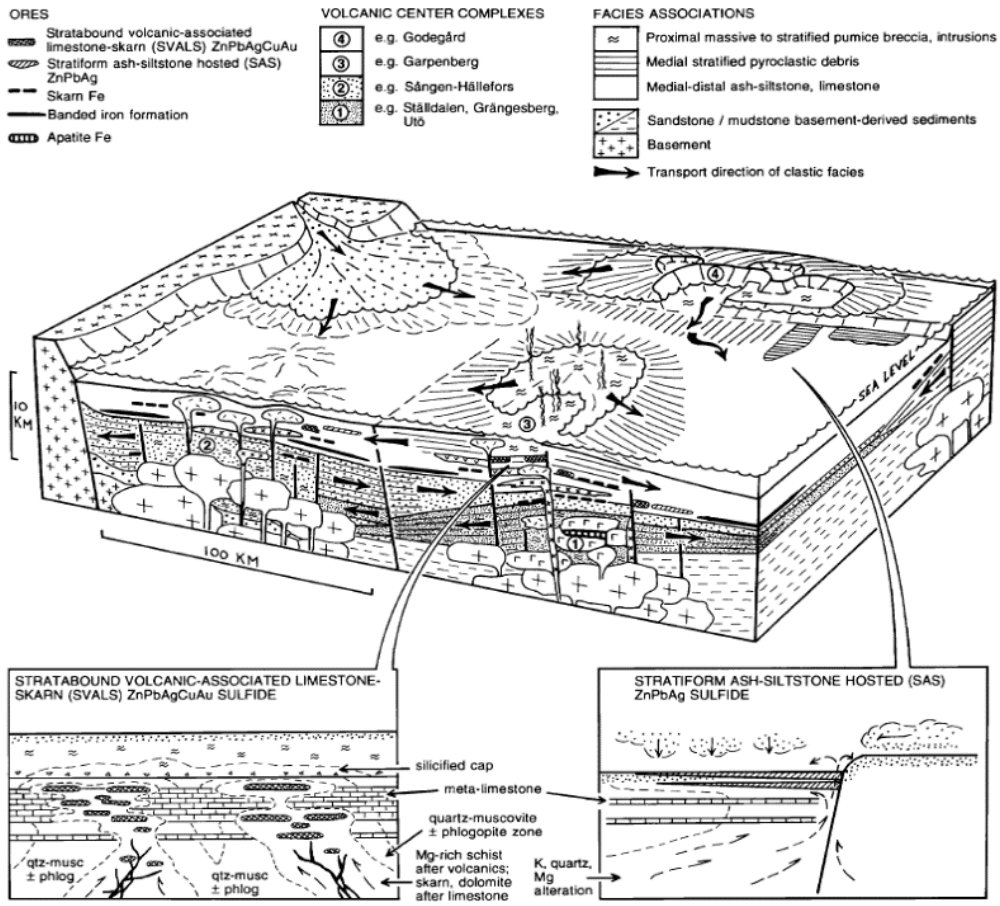

Appendix B. Coordinates of collected brucite samples in field (Sweref 99 1330).

Sample ID	*Y (latitude)*	*X (longitude)*	*Z (altitude)*
FS15	*6623927.936*	*191313.773*	*195.830*
FS25	*6624100.956*	*191320.645*	*197.834*
FS44	*6624495.769*	*190892.542*	*176.095*
FS92a	*6624199.147*	*191117.238*	*178.415*
FS92c	*6624196.796*	*191120.101*	*178.987*

Appendix C. 3D-modelled brucite distribution with moderate (yellow) and high (red) quantities of brucite, viewed from east. (Rotated image towards left).

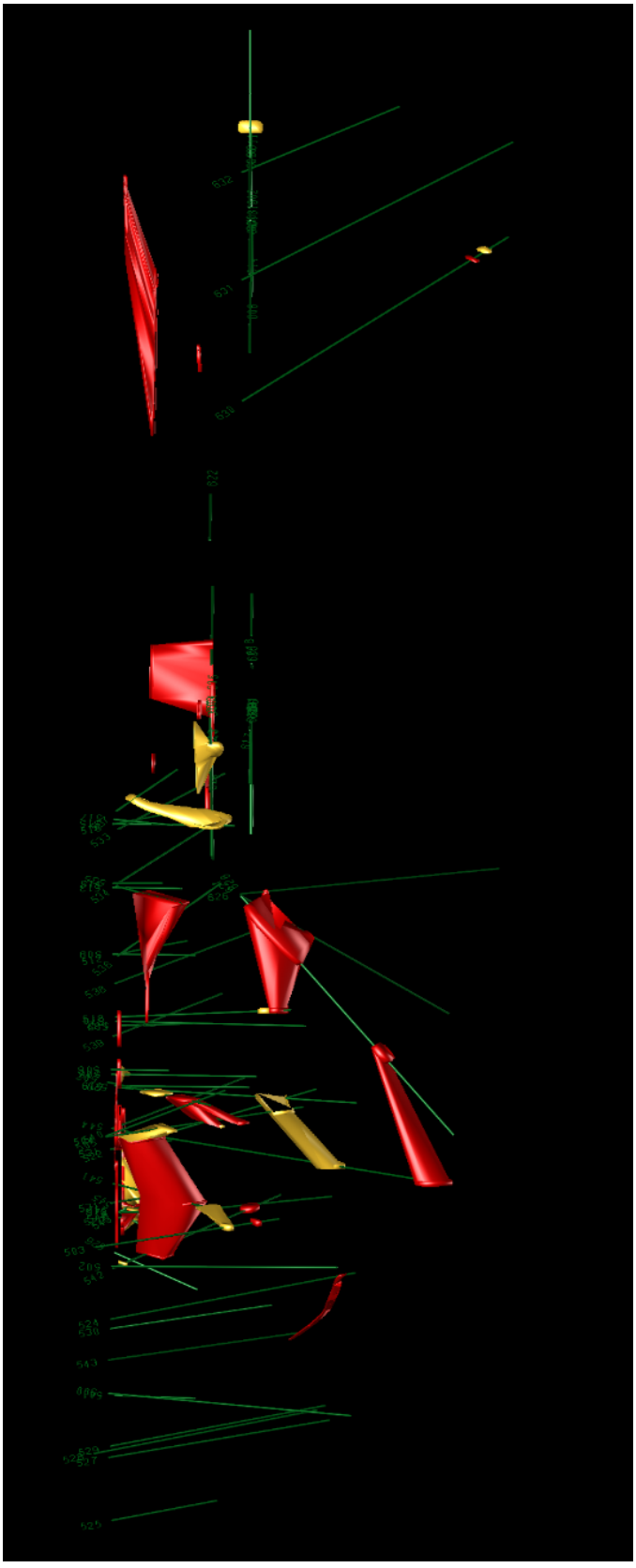

Appendix D. 3D-model of brucite mineralization in the Gåsgruvan quarry with all associated mineralizations. Blue = amphibolite, yellow = felsic metavolcanite, dark green = skarn. (Rotated image towards left).

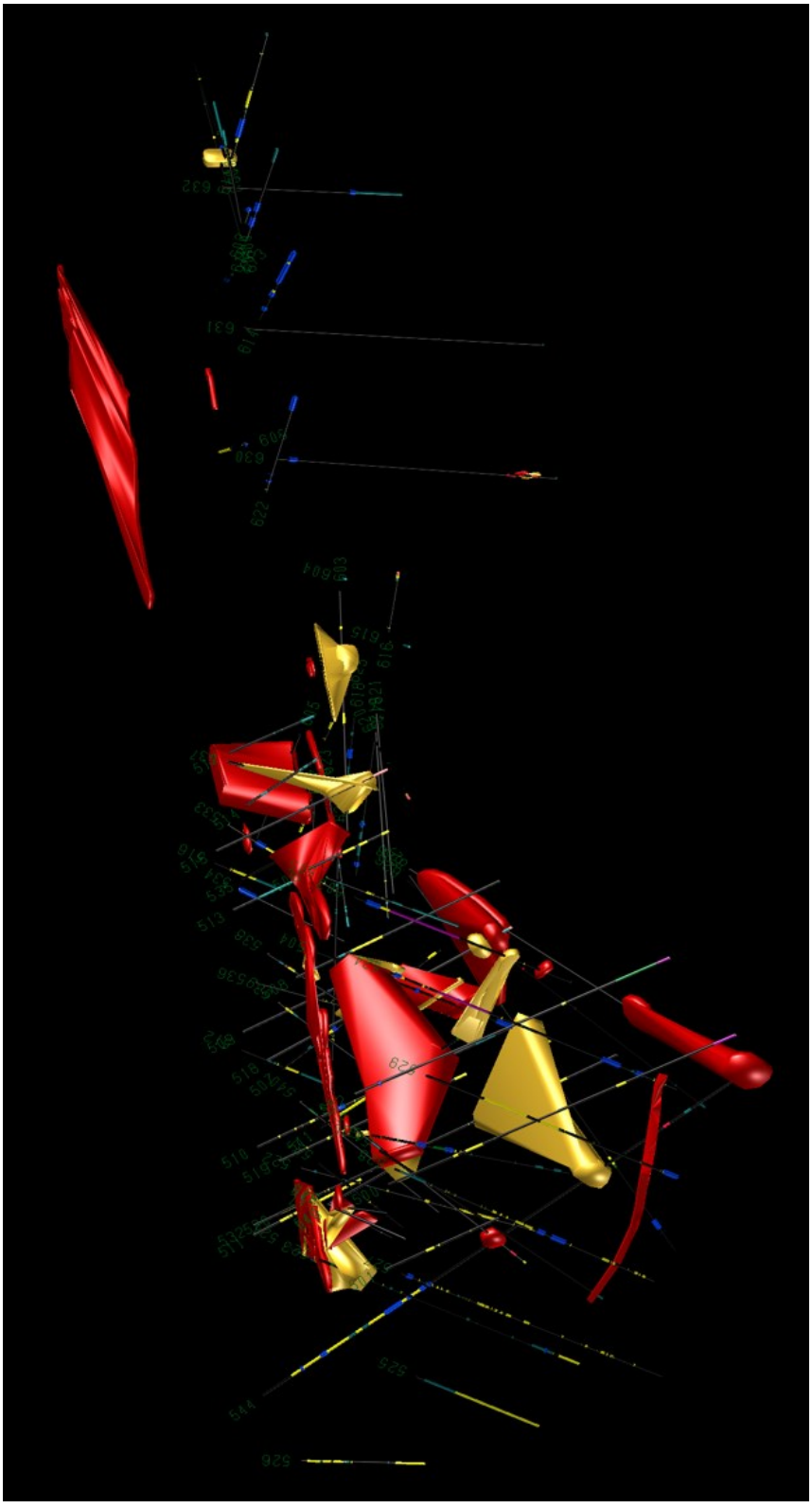

Appendix E. SEM-EDS analysis results

SEM-EDS analysis results, sample FS15

(Fig. 27c)

	C	O	F	Mg	Al	Si	Ca	Mn	Fe
1	3.11	34.33		15.29	1.5		3.18	4.09	38.49
2	3.96	43.17		19.52	21.34		3.14		8.88
3	3.21	47.84		37.13			3.22		8.59
4	0.02	47.94		22.87			19.17		
5	5.13	43.15	2.05	32.17		12.08	5.42		
Average	5.09	43.29	2.05	25.39	11.42	12.08	6.83	4.09	18.65
Deviation	2.87	5.54	0	9.04	14.03	0	6.97	0	17.18

SEM-EDS analysis results, sample FS25

(Fig. 28a)

	C	O	Mg	Ca	Mn	Fe
1	3,06	32,23	15,07	2,68	4,49	42,48
2		53,03	42,99	3,98		
3	12,93	50,45	16,13	20,5		
Average	7,99	45,23	24,73	9,05	4,49	42,48
Deviation	6,98	11,34	15,83	9,93	0	0

(Fig. 28b)

	C	O	Mg	Al	Ca	Mn	Fe
1	4,22	53,45	40,01		2,32		
2	3,42	30,93	14,48	0,82	2,42	3,85	44,09
3	4,14	50,4	39,64		2		3,82
Average	3,93	44,93	31,38	0,82	2,25	3,85	23,95
Deviation	0,44	12,22	14,63	0	0,22	0	28,47

	C	O	Mg	Ca
1	5,27	53,26	37,39	4,08
2	13,71	49,98	15,09	21,22
3	12,05	49	3,81	35,13
Average	10,35	50,75	18,76	20,14
Deviation	4,47	2,23	17,08	15,55

SEM-EDS analysis results, sample DC503.13

(Fig. 31a)

	C	O	Mg	Si	Ca	Mn	Fe
1	13,05	46,53	5,79	0,32	30,68		3,62
2	8,09	26,39	6,73	0,39	1,55	1,14	55,72
3	9,56	48,77	35,41	0,94	1,46		3,85
Average	10,23	40,56	15,98	0,55	11,23	1,14	21,07
Deviation	2,55	12,33	16,83	0,34	16,85	0	30,01

	C	O	Mg	Si	Ca	Mn	Fe
1	7,93	31,21	12,53		1,25		47,08
2	7,51	30,06	12,01		1,32	2,71	46,38
3	14,45	31,6	11,66	0,28	1,34	3,71	36,97
4	8,39	28,81	11,44		1,46	1,61	48,29
Average	9,57	30,42	11,91	0,28	1,34	2,68	44,68
Deviation	3,27	1,25	0,47	0	0,08	1,05	5,2

SEM-EDS analysis results, sample DC515.65

(Fig. 33b)

	C	O	Mg	Al	Si	Ca	Ti	Fe
1	4,27	31,01	12,88	1,07	2,36	1,51	1,09	45,81
2	7,7	43,63	32,63		14,02	2,02		
3	10,21	52,64	32,84		0,53	3,78		
4	5,81	31,53	11,53			3,29	0,82	47,03
5	13,43	47,9	4,83		0,88	32,95		
6	14,1	50,44	15,82		0,61	19,03		
Average	9,25	42,86	18,42	1,07	3,68	10,43	0,95	46,42
Deviation	4,02	9,47	11,66	0	5,83	12,86	0,19	0,86

SEM-EDS analysis results, sample DC518.13

(Fig. 34b)

	C	O	Mg	Al	Si	Ca	Fe
1	3,62	28,01	4,75		2,36	4,01	57,25
2	12,71	47,78	6,03	0,28	3,4	29,8	
3	4,22	49,37	24,9	1,99	16,31	3,21	
Average	6,85	41,72	11,9	1,14	7,36	12,34	57,25
Deviation	5,08	11,9	11,28	1,21	7,77	15,13	0